

THS



This is to certify that the

thesis entitled A SIMILARITY SOLUTION OF A SECOND-ORDER MODEL OF FREE TURBULENT JETS WITH A PASSIVE SCALAR CONTAMINANT AND ITS APPLICABILITY TO TWO-PHASE JETS

presented by

Brian Ronald Cunningham

has been accepted towards fulfillment of the requirements for

M. S. degree in Chemical Engineering

Major professor

O-7639



OVERDUE FINES: 25¢ per day per item

RETURNING LIBRARY MATERIALS:

Place in book return to remove charge from circulation records

A SIMILARITY SOLUTION OF A SECOND-ORDER MODEL OF FREE TURBULENT JETS WITH A PASSIVE SCALAR CONTAMINANT AND ITS APPLICABILITY TO TWO-PHASE JETS

Ву

Brian Ronald Cunningnam

A THESIS

Submitted to

Michigan State University
in partial fulfillment of the requirements
for the degree of

MASTER OF SCIENCE

Department of Chemical Engineering

1980

ABSTRACT

A SIMILARITY SOLUTION OF A SECOND-ORDER MODEL OF FREE TURBULENT JETS WITH A PASSIVE SCALAR CONTAMINANT AND ITS APPLICABILITY TO TWO-PHASE JETS

By

Brian Ronald Cunningham

In this thesis, a second-order model of turbulence is described for free turbulent axial jets. Differential transport equations for the Reynolds shear stress, the turbulence kinetic energy, and the dissipation of energy are employed. Additional transport equations for the mean concentration and the square of the root-mean-square concentration fluctuations of a passive scalar contaminant are also used. The equations are reduced to their similarity form in plane and axisymmetric jets and solved numerically.

Possible additions to the model to approximate the behavior of two-phase jets are discussed and a survey of the literature on two-phase jets is presented.

TABLE OF CONTENTS

													Page
LIST O	F TABLES .			•	•	•	•	•	•	•	•	•	iii
LIST O	F FIGURES			•	•	•	•	•	•	•	•	•	iv
Section	n												
I.	INTRODUCT	rion .		•	•	•	•	•	•	•	•	•	1
II.	THE NEED	TO MOI	DEL	•	•	•	•	•	•	•	•	•	3
III.	DEVELOPME	ENT OF	THE	MODE	EL	•	•		•	•	•	•	7
IV.	REDUCTION	OF TH	HE MO	DDEL	TO	SI	MIL	ARI	ΓY	FOR	M	•	17
v.	RESULTS A	AND DIS	cus	SION	•	•	•	•	•	•	•	•	32
VI.	TWO-PHASE	E JETS	•	•	•	•	•	•	•	•	•	•	45
VII.	CONCLUSIO	ONS AND	REC	COMMI	END	TI	SNC		•	•	•	•	55
REFERE	VCES												5.8

LIST OF TABLES

Table				Page
1.	Sensitivity of the spreading rate on \mathcal{C}_{C1} , \mathcal{C}_{k} , and \mathcal{C}_{62}	•		33
2.	Sets of constants evaluated	•	•	33
3.	Constants used in the model equations for the passive contaminant properties		•	36

LIST OF FIGURES

Fi	.gure		Page
	1.	The τ -k- ε model	13
	2a.	The model equations written for the plane jet	16
	25.	The model equations written for the axisymmetric jet	16
	3.	Some properties of the axial jet in the region of similarity	18
	4.	The similarity equations to be solved for the contaminated plane jet	22
	5.	The additional similarity equations to be solved for the contaminated plane jet	25
	6.	The similarity equations to be solved for the uncontaminated axisymmetric jet	28
	7.	The additional similarity equations to be solved for the contaminated axisymmetric jet	30
	8.	Comparison of predictions of the mean axial velocity and mean contaminant concentration profiles in the plane jet with experimental data	40
	9.	Comparison of predictions of the turbu- lence of kinetic energy and the square of the root-mean-square contaminant concentration fluctuations in the plane jet with experimental data	41
1	.0.	Comparison of predictions of the mean axial velocity and mean contaminant concentration profiles in the axisymmetric jet with experimental data	42

Figure				Page
11.	Comparison of the prediction of the turbulence kinetic energy with experimental data and the prediction of the square of the root-mean-square contaminant concentration fluctuations in the axisymmetric jet		•	43
12.	Comparison of the prediction of the normalized square of the root-mean-square contaminant concentration fluctuations in the axisymmetric jet with experimental data	•	•	44

I. INTRODUCTION

The renewed interest in coal as an energy source, along with increased environmental restrictions on its use, has initiated several technical problems. Two of the more obvious problems to be solved are the needs for efficient designs of the combustion chamber for the pulverized coal and the cleaning system for the stack gases. In order to obtain a better design for these devices, a more complete understanding of the turbulent flow fields present within them than currently exists is desirable.

The turbulence in the above examples consists of two phases, a continuous fluid (gaseous) phase and a discrete particulate phase. A common method of mixing the pulverized coal with air in combustion chambers is to use axial jets issuing from injection nozzles. Because of this, and the sufficient literature available on measurements of velocity and concentration profiles within axial, free turbulent jets, a model for both planar and axisymmetric geometries of this type of jet has been chosen for study here.

Initially, the model is developed for a singlephase jet, along with the equations required to describe
the behavior of a passive scalar contaminant within the

jet. Examples of such a contaminant include the addition of another gaseous compound or a temperature difference between the entering jet fluid and the ambient fluid such that bouyancy effects are negligible. In a later section, possible additions to the model to accommodate the effects of a two-phase flow will be discussed.

The following section describes the difficulty encountered in solving the exact equations governing the jet and the subsequent necessity to model certain terms appearing in the equations. In Section III, the model for the single-phase jet is developed. Section IV deals with the reduction of the model equations to their form in the self-preserving, or similarity, region of the jet along with the appropriate boundary conditions. Although this region of the jet is not the focus of attention for coal combustion chambers, most of the reported data is presented in this region. In addition, the partial differential equations of the model are reduced to ordinary differential equations, thereby simplifying their solution.

The results of the calculations using the selfpreserving form of the model are then presented in Section V
and compared to experimental data found in the literature.
A review of the literature on two-phase jets follows in
Section VI. Finally, conclusions are drawn and recommendations for further studies are proposed in Section VII.

II. THE NEED TO MODEL

The mathematical description of the conservation of momentum for a fluid of constant density, ρ , and viscosity, μ , is given by the Navier-Stokes equations as

$$\rho \frac{\partial \vec{u}}{\partial t} + \rho u_j \frac{\partial \vec{u}}{\partial z_j} = -\nabla P + \mu \nabla^2 \vec{u} + \rho \vec{g}$$
 (2.1)

and the equation of continuity

$$\nabla \cdot \vec{\mu} = 0. \tag{2.2}$$

For a fluid in turbulent flow, the most understandable approach for working towards a solution to the equations is to consider each of the instantaneous velocity components, U_j , to be composed of a time-steady component, \bar{U}_j , and a fluctuating velocity component around \bar{U}_j , v_j . Thus, $v_j = \bar{U}_j + v_j$ with $\bar{v}_j = \bar{U}_j$ and $\bar{v}_j = 0$, where the overbar represents averaging with respect to time. This technique was first proposed by Reynolds and is known as a Reynolds decomposition.

Upon substitution of this convention into (2.1) and (2.2), using the continuity equation and taking the time-average of (2.1), it is readily seen that the resulting equation for the mean velocity contains the gradient of the double velocity correlation $\overrightarrow{u_i'u_i'}$ arising from the non-

linear term in (2.1). Consequently, it is necessary to develop additional relations describing the behavior of the $\overline{u_i'u_j'}$ within the jet. In this study, transport equations obtained through manipulations of the Navier-Stokes equations are developed for each of the $\overline{u_i'u_j'}$.

However, once this is done, it is seen that these equations contain triple velocity (third order) correlations, $\overline{u_i^*u_j^*u_k^*}$. This trend continues in the transport equations for the third and higher order terms so that the system of equations and unknowns can never be closed. Consequently, a unique, exact solution of the equations is impossible. A closure hypothesis is therefore assumed so that a unique solution can be found. That is, the assumption is made that the higher order terms are described by known functions of the lower order modelling variables.

An example of a first order closure is given by the eddy viscosity for the Reynolds shear stress Υ (= $\overrightarrow{u_i}.\overrightarrow{u_i'}$) as

$$T = -\mu_{e} \frac{\partial \tilde{\mu}}{\partial \tilde{y}} \tag{2.3}$$

where μ_t is the eddy viscosity. This modelling scheme draws an analogy between the viscous shear stress in a Newtonian fluid and the turbulence shear stress. The only difference is that the eddy viscosity is not an intrinsic property of the fluid, but a property of the flow and may vary across the jet.

In this study, a second order closure is employed and transport equations for terms of higher order than the $\widehat{u_i'u_j'}$ are not developed. However, it is noted from previous works using each of the $\widehat{u_i'u_j'}$ separately [c.f. Wood (1978)], that the normal stresses are of the same order of magnitude and behave similarly. As a result of this, the normal stresses are not considered separately here but are summed and only equations for the turbulence shear stress, \mathcal{T} , and the turbulence kinetic energy, $k(\mathbf{r} \vdash_{\mathcal{T}} \widehat{u_i'}\widehat{u_i'})$, are used.

In any modelling scheme for free turbulent jets, expressions for a velocity scale and a length scale are required. In some of the simpler models [c.f. Reynolds (1976)], the length scale may be given by an algebraic expression. In this study, the length scale is given implicitly through the dissipation of the kinetic energy, ϵ . The dissipation occurs primarily at the smallest scales of the turbulence which at high Reynolds numbers may be assumed to be locally isotropic. It has been shown for isotropic turbulence [Hinze (1975)] that the dissipation is proportional to $u^3/2$, where ℓ is the characteristic length scale of the turbulence. A transport equation for $\epsilon(\epsilon \nu \frac{\partial U}{\partial \Sigma_i} \frac{\partial U}{\partial \Sigma_j})$ can also be obtained through manipulations of (2.1). Thus, the model used in this study is a $\tau k - \epsilon$, or three-equation, model since differential transport

equations are employed for the three turbulence quantities mentioned above.

Because the behavior of a two-phase jet is an important but not well-understood application of turbulence modelling, the profiles of a passive scalar contaminant mean concentration and its root-mean-square fluctuations are modelled as being an asymptotic limit of the particulate profile in a two-phase jet as the size and loading of the particles tend to zero. Thus, differential equations are developed to describe the transport of a passive contaminant as well.

III. DEVELOPMENT OF THE MODEL

The equation for the mean velocity in a jet at high Reynolds numbers can be obtained from equation (2.1) after a Reynolds decomposition and time averaging as

$$\bar{U}_{\mathbf{k}} \frac{\partial \bar{U}_{i}}{\partial x_{\mathbf{k}}} = -\frac{\partial}{\partial x_{\mathbf{k}}} (\bar{u}_{i}' \bar{u}_{\mathbf{k}}'). \tag{3.1}$$

To obtain an equation for $u_i^{\prime}u_j^{\prime}$, (2.1) written in the i-direction, multiplied by u_i^{\prime} is added to (2.1) written in the j-direction multiplied by u_i^{\prime} . After liberal use of the continuity equation and time-averaging, the resulting equation may be written as

$$\widetilde{U}_{k} \frac{\partial}{\partial x}_{k} \left(\overline{u_{i}' u_{j}'} \right) = -\left(\overline{u_{j}' u_{k}'} \frac{\partial \widetilde{U}_{i}}{\partial x_{k}} + \overline{u_{i}' u_{k}'} \frac{\partial \widetilde{U}_{j}}{\partial x_{k}} \right) - 2\nu \left(\frac{\partial \overline{u_{i}'}}{\partial x_{k}} \frac{\partial U_{j}'}{\partial x_{k}} \right) + \frac{\gamma}{9} \left(\frac{\partial u_{i}'}{\partial x_{j}} + \frac{\partial u_{i}'}{\partial x_{i}} \right) \\
- \frac{\partial}{\partial x}_{k} \left(\overline{u_{i}' u_{j}' u_{k}'} - \left[\nu_{Sx} \left(\overline{u_{i}' u_{j}'} \right) - \frac{\gamma}{9} \left(\delta_{ik} u_{j}' + \delta_{jk} u_{i}' \right) \right] \right). \tag{3.2}$$

Since only high Reynolds number jets are being considered here, the dissipation occurring mainly at the small scales (term b) can be written as

$$-2\nu\left(\frac{\partial u_{i}^{2}}{\partial x_{k}}\frac{\partial u_{i}^{2}}{\partial x_{k}}\right) = -\frac{2}{3}\delta_{ij} \mathcal{E}$$
(3.3)

because the small scales can be assumed to exhibit local isotropy. The viscous and pressure diffusion (term e) may be neglected as another result of high Reynolds number flow.

The pressure-strain correlation (term c) can be broken into two parts [Launder, Reece, and Rodi (1975)], the first being a result of fluctuating quantities and the second arising from the interaction of the mean rate of strain and turbulence fluctuations as

$$\frac{\vec{j}(\frac{\partial u_i}{\partial x_i} + \frac{\partial u_j}{\partial x_i}) = (\phi_{ij} + \phi_{ji})_{,i} + (\phi_{ij} + \phi_{ji})_{,2}.$$
(3.4)

The first term is almost universally modelled as

$$(\phi_{ij} + \phi_{ji})_{,i} = -C_i \frac{\varepsilon}{R} \left(\overline{u_i' u_j'} - \frac{2}{3} S_{ij} R \right)_{,i}$$
(3.5)

where c_1 is a constant. Since this term is zero for isotropic turbulence and is linear in the departure from isotropy, it tends to make the components of the Reynolds stress tensor isotropic. The term related to the mean rate of strain has been modelled by Launder, Reece, and Rodi (1975) as

$$(\phi_{ij} + \phi_{ji})_{,2} = -\gamma_{p} (P_{ij} - \frac{2}{3} S_{ij} P)$$
 (3.6)

where

$$P_{ij} = -\left(\overline{u_i'u_k'} \frac{\partial \overline{u_i}}{\partial x_k} + \overline{u_j'u_k'} \frac{\partial \overline{u_i'}}{\partial x_k}\right),$$

P is the rate of production of turbulence kinetic energy $(= \frac{1}{2}P_{11})$, and $\stackrel{\vee}{V}_{p}$ is a constant. The pressure-strain correlation is also zero for isotropic turbulence.

Since a second order closure is being used, the gradient diffusion (term d) triple correlation must be modelled in terms of the second and lower order modelling variables. It is noted that the correlation $\widehat{u_i'u_j'u_k'}$ is a third order tensor symmetric in i, j, and k so any model for this term must also display this characteristic. The approximation

$$-\overline{u_{i}^{\prime}u_{j}^{\prime}u_{k}^{\prime}} = C_{s} \frac{k}{\varepsilon} \left[\overline{u_{i}^{\prime}u_{k}^{\prime}} \frac{\partial (\overline{u_{i}^{\prime}u_{k}^{\prime}})}{\partial x_{j}} + \overline{u_{j}^{\prime}u_{k}^{\prime}} \frac{\partial (\overline{u_{i}^{\prime}u_{k}^{\prime}})}{\partial x_{j}} + \overline{u_{k}^{\prime}u_{k}^{\prime}} \frac{\partial (\overline{u_{i}^{\prime}u_{k}^{\prime}})}{\partial x_{j}} \right]$$

$$(3.7)$$

proposed by Launder, Reece, and Rodi (1975) satisfies the above condition and is adopted here.

Thus, equation (3.2) may now be written in its modelled form as

$$\widetilde{U}_{\mathbf{k}} \frac{\partial}{\partial x_{\mathbf{k}}} \left(\overline{u_{i}^{\prime} u_{i}^{\prime}} \right) = -\left(\overline{u_{i}^{\prime} u_{\mathbf{k}}^{\prime}} \frac{\partial \widetilde{u}_{i}}{\partial x_{\mathbf{k}}} + \overline{u_{i}^{\prime} u_{i}^{\prime}} \frac{\partial \widetilde{u}_{i}}{\partial x_{\mathbf{k}}} \right) - \frac{2}{3} \delta_{ij} \varepsilon - C_{i} \frac{\varepsilon}{h} \left(\overline{u_{i}^{\prime} u_{i}^{\prime}} - \frac{2}{3} \delta_{ij} h \right) - \lambda_{i} \left(P_{ij} - \frac{2}{3} \delta_{ij} P \right) \\
- \frac{\partial}{\partial x_{\mathbf{k}}} \left(-C_{i} \frac{h}{\varepsilon} \left[\overline{u_{i}^{\prime} u_{i}^{\prime}} \frac{\partial \overline{u_{i}^{\prime} u_{i}^{\prime}}}{\partial x_{\mathbf{k}}} + \overline{u_{i}^{\prime} u_{i}^{\prime}} \frac{\partial \overline{u_{i}^{\prime} u_{i}^{\prime}}}{\partial x_{\mathbf{k}}} + \overline{u_{\mathbf{k}}^{\prime} u_{i}^{\prime}} \frac{\partial \overline{u_{i}^{\prime} u_{i}^{\prime}}}{\partial x_{\mathbf{k}}} \right) \right] \right) \tag{3.8}$$

The model transport equation for the turbulence shear stress T (= $u_i'u_1'$) is obtained from equation (3.8) by setting i=1 and j=2. Because of boundary layer assumptions, cross-stream gradients are much greater than the streamwise gradients, the $\frac{\partial}{\partial x_i}$ terms are neglected on the R.H.S. of (3.8). Also, $\frac{\partial \bar{u}_i}{\partial x_i} >> \frac{\partial \bar{u}_i}{\partial x_i}$ so that the equation for T may be written as

$$\bar{U}_{\mathbf{k}} \frac{\partial T}{\partial \mathbf{x}_{\mathbf{k}}} = -C_{\mathbf{n}} \mathbf{k} \frac{\partial \bar{U}_{\mathbf{k}}}{\partial \mathbf{x}_{\mathbf{k}}} - C_{\mathbf{T} \mathbf{k}} \frac{\mathbf{E} T}{\mathbf{k}} + C_{\mathbf{T}} \frac{\partial}{\partial \mathbf{x}} \left(\frac{\mathbf{k}^{2}}{\mathbf{E}} \frac{\partial T}{\partial \mathbf{x}_{\mathbf{k}}} \right) (3.9)$$

ADVECTION = PRODUCTION - DISSIPATION + DIFFUSION where it is noted that $\overrightarrow{u_1'v_2'}$ $\{k\}$ and the assumption is made that the "diffusion" of the shear stress depends only on the gradient of the shear. In the region of the crosssection of the jet where advection and diffusion balance each other, (3.9) can be solved for as

$$\gamma = -\left(\frac{C_{71}}{C_{72}}\right) \frac{k^2}{\varepsilon} \frac{\partial \bar{U}}{\partial z},$$
(3.10)

which is recognized as the same form as equation (2.3) where $^{1/2}$ behaves as an eddy viscosity. Most two-equation models, which solve differential transport equations only for the turbulence velocity and length scales and use an equation of the form of (2.3) for the turbulence shear stress [Rodi and Spalding (1970)] instead of a differential equation for (2.3) such as (3.9).

The model transport equation for the turbulence kinetic energy $k (: :_2 \overline{\nu_i \cdot \nu_i'})$ is also obtained from equation (3.8). By setting j = i and making the corresponding assumptions made in the τ equation, the result is

$$\bar{U}_{k}\frac{\partial k}{\partial x_{k}} = -T\frac{\partial \bar{U}}{\partial x_{k}} - \varepsilon + C_{k}\frac{\partial}{\partial x_{k}} \left(\frac{k^{2}}{\varepsilon}\frac{\partial k}{\partial x_{k}}\right). \tag{3.11}$$

The derivation of the dissipation equation is similar to that of equation (3.2) but with (2.1) written in the i-direction and differentiated with respect to χ_{ℓ} before being multiplied by $\nu \frac{\partial \mathcal{U}}{\partial x_{\ell}}$. The resulting equation is given by

$$\tilde{U}_{k} \frac{\partial \mathcal{E}}{\partial x_{k}} = \left(\nu \frac{\partial^{2} \mathcal{E}}{\partial x_{k} \partial x_{k}} - 2\nu \frac{\partial^{2} \tilde{U}_{i}}{\partial x_{k} \partial x_{i}} \left(u_{k}^{i} \frac{\partial U_{i}^{i}}{\partial x_{k}} \right) \right) - 2\nu \frac{\partial \tilde{U}_{i}}{\partial \tilde{x}_{k}} \left(\frac{\partial \tilde{U}_{i}^{i} \partial U_{i}^{i}}{\partial x_{k} \partial x_{i}} + \frac{\partial u_{i}^{i} \partial u_{k}^{i}}{\partial x_{k} \partial x_{k}} \right) \\
- 2\nu \left(\frac{\partial u_{i}^{i}}{\partial x_{k}} \frac{\partial U_{i}^{i}}{\partial x_{k}} \frac{\partial u_{k}^{i}}{\partial x_{k}} \right) - \nu \frac{\partial}{\partial x} \left(u_{k}^{i} \frac{\partial u_{i}^{i}}{\partial x_{k}} \frac{\partial u_{i}^{i}}{\partial x_{k}} \right) - 2 \frac{\nu}{p} \frac{\partial}{\partial x_{i}} \left(\frac{\partial u_{i}^{i}}{\partial x_{k}} \frac{\partial P_{i}^{i}}{\partial x_{k}} \right) \\
- 2\nu^{2} \left(\frac{\partial^{2} u_{i}^{i}}{\partial x_{k} \partial x_{k}} \right)^{2}. \tag{8}$$

Term (a) of (3.12) is recognized as being important only in low Reynolds number flows and is neglected in further considerations.

Following Hanjalic and Launder (1972), term (b), upon contraction of the indices, yields components of the dissipation and their approximation

$$2\nu \frac{\partial \bar{u}_{i}}{\partial x_{k}} \left(\frac{\partial u_{i}}{\partial x_{k}} \frac{\partial u_{i}}{\partial x_{i}} + \frac{\partial u_{i}}{\partial x_{k}} \frac{\partial u_{i}}{\partial x_{k}} \right) = C_{\varepsilon_{i}} \frac{\varepsilon}{k} \overline{u_{i}'u_{k}'} \frac{\partial \bar{u}_{i}}{\partial x_{k}}$$
(3.13)

is adopted. For sufficiently high Reynolds numbers, terms (c) and (f) may be considered together as being characteristic of the cascade of energy from the large to the dissipative small scales of the turbulence. As such, the modelling approximation should be independent of the viscosity of the fluid. The suggestion of Hanjalic and Launder (1972) that

$$2\nu\left(\frac{\partial u_{i}^{\prime}}{\partial x_{2}}\frac{\partial u_{i}^{\prime}}{\partial x_{k}}\frac{\partial u_{k}^{\prime}}{\partial x_{2}}\right)+2\nu^{2}\left(\frac{\partial^{2}u_{i}^{\prime}}{\partial x_{k}\partial x_{2}}\right)^{2}=C_{\ell 2}\frac{\varepsilon^{2}}{k}$$
(3.14)

is accepted. Term (d) can be interpreted as the diffusion due to velocity fluctuations of the dissipation. As in term (d) of equation (3.2) this term is also tensor symmetric and the modelling can be accomplished similar to the previous cases. Additional simplifications can be made beyond those for (3.7), however, so that the resulting approximation is

$$-\nu \frac{\partial}{\partial x_{h}} \left(u_{h}^{i} \frac{\partial u_{i}^{i}}{\partial x_{h}} \frac{\partial u_{i}^{i}}{\partial x_{h}} \right) = C_{\varepsilon} \frac{k}{\varepsilon} u_{h}^{i} u_{i}^{j} \frac{\partial \varepsilon}{\partial x_{h}}. \tag{3.15}$$

Term (e) represents the diffusion of the dissipation caused by pressure fluctuations. Although modelling of this term results in a form similar to (3.4), the terms contain higher order derivatives than previously encountered. Therefore, accepting the suggestion of Hanjalic and Launder (1972), this term will be neglected.

The modelled transport equation for the dissipation of kinetic energy can now be written as

$$\bar{U}_{\mathbf{k}} \frac{\partial \mathcal{E}}{\partial x_{\mathbf{k}}} = -C_{\mathbf{\epsilon}_{1}} \frac{\mathcal{E}^{T}}{\mathbf{k}} \frac{\partial \bar{U}}{\partial x_{\mathbf{k}}} - C_{\mathbf{\epsilon}_{2}} \frac{\mathcal{E}^{2}}{\mathbf{k}} + C_{\mathbf{\epsilon}_{2}} \frac{\partial}{\partial x_{\mathbf{k}}} \left(\frac{\mathbf{k}^{2}}{\mathbf{\epsilon}} \frac{\partial \mathcal{E}}{\partial x_{\mathbf{k}}} \right), \tag{3.16}$$

where the assumptions made in the development of the τ and k equations are applied here as well. Figure 1

summarizes the τ -k- ε model written in the form of ADVECTION = PRODUCTION - DISSIPATION + DIFFUSION.

ADVECTION = PRODUCTION - DISSIPATION + DIFFUSION
$$\bar{U}_{k} \frac{\partial \bar{I}}{\partial x_{k}} = -c_{T_{1}} k \frac{\partial \bar{U}}{\partial x_{2}} - c_{T_{2}} \frac{\varepsilon \bar{I}}{k} + c_{T} \frac{\partial}{\partial x_{2}} (\frac{k}{\varepsilon} \frac{\partial \gamma}{\partial x_{2}})$$

$$\bar{U}_{k} \frac{\partial k}{\partial x_{k}} = -\gamma \frac{\partial \bar{U}}{\partial x_{2}} - \varepsilon + c_{k} \frac{\partial}{\partial x_{2}} (\frac{k}{\varepsilon} \frac{\partial k}{\partial x_{2}})$$

$$\bar{U}_{k} \frac{\partial \varepsilon}{\partial x_{k}} = -c_{\varepsilon_{1}} \frac{\varepsilon \bar{I}}{k} \frac{\partial \bar{U}}{\partial x_{2}} - c_{\varepsilon_{2}} \frac{\varepsilon^{2}}{k} + c_{\varepsilon} \frac{\partial}{\partial x_{2}} (\frac{k}{\varepsilon} \frac{\partial \varepsilon}{\partial x_{2}})$$

Figure 1.—The $\tau - k - \varepsilon$ Model.

In addition to the model for an uncontaminated jet, a model for the mean concentration and the root-mean-square concentration fluctuations of a passive scalar contaminant are desired as well. Such a contaminant could be an additional fluid-phase compound of the same density as the jet fluid or a temperature field within the jet, provided any bouyancy effects are negligible. It is hoped that the predictions obtained will be useful for future applications in dilute solutions of two-phase flows.

The instantaneous scalar field in a steady flow is given, upon a Reynolds decomposition, by

$$(\bar{\mathcal{U}}_{\mathbf{k}} + \mathcal{U}_{\mathbf{k}}') \frac{\partial}{\partial x_{\mathbf{k}}} (\hat{\Theta} + \Theta') = \lambda \frac{\partial^{2}}{\partial x_{\mathbf{k}}} \frac{\partial}{\partial x_{\mathbf{k}}} (\hat{\Theta} + \Theta'), \tag{3.17}$$

where the instantaneous concentration is given by $\theta = \bar{\theta} + \theta'$ as in the velocity and δ' is the molecular diffusion coefficient for θ . An equation for the mean concentration profile is obtained by time-averaging (3.17) and is given by

$$\overline{U}_{k} \frac{\partial \overline{\Theta}}{\partial x_{k}} + \frac{\partial}{\partial x_{k}} (\overline{u_{k}'\Theta'}) = \sqrt[3]{\frac{\partial^{2} \overline{\Theta}}{\partial x_{k} \partial x_{k}}}. \tag{3.18}$$

At high Reynolds numbers, the molecular diffusion of the contaminant is negligible relative to the turbulent flux $\widehat{u_k'}$ of and is left out of further considerations. Again, the streamwise derivative of the turbulent flux is much less than the cross-stream derivative and is also neglected.

Following the work of Spalding (1971), the turbulence flux can be modelled by a transport hypothesis as

$$\overline{U_{2}'\Theta'} = -\frac{1}{c_{ir}} \frac{\overline{U_{2}'U_{2}'}}{k} \frac{k^{2}}{\epsilon} \frac{\partial \bar{\Theta}}{\partial x_{2}} = -C_{\Theta} \frac{k^{2}}{\epsilon} \frac{\partial \bar{\Theta}}{\partial x_{2}}$$
(3.19)

which fits the form of an eddy viscosity divided by a turbulent Schmidt number multiplying the gradient of the mean concentration. This is analogous to the eddy viscosity model [equation (3.10)] for the turbulence

shear stress, $\overline{\mathcal{U}_1'\mathcal{U}_2'}$. Thus, the model equation for the mean concentration profile is

$$\bar{U}_{k} \frac{\partial \bar{\Theta}}{\partial x_{k}} = C_{\Theta} \frac{\partial}{\partial x_{k}} \left(k \frac{\partial \bar{\Theta}}{\bar{E}} \frac{\partial \bar{\Theta}}{\partial x_{k}} \right). \tag{3.20}$$

The equation for the root-mean-square of the fluctuations is obtained by multiplying equation (3.17) by Θ' and then time-averaging. This results in

$$\bar{U}_{\mathbf{k}} \frac{\partial (\overline{\Theta'\Theta'})}{\partial x_{\mathbf{k}}} = 2\delta \left(\overline{\Theta'} \frac{\partial^2 \Theta'}{\partial x_{\mathbf{k}}} \right) - 2 \overline{u_{\mathbf{k}}'\Theta'} \frac{\partial \overline{\Theta}}{\partial x_{\mathbf{k}}} - \frac{\partial}{\partial x_{\mathbf{k}}} \left(\overline{u_{\mathbf{k}}'(\Theta'\Theta')} \right). \tag{3.21}$$

Using the previous model for $\widehat{\nu_{\!\!4}'e'}$ and an analogous substitution for $\widehat{\nu_{\!\!4}'(e'e')}$, along with a dissipation hypothesis as presented by Spalding (1971) given as

$$\mathcal{J}\left(\Theta'\frac{\partial^2 \Theta'}{\partial x_k \partial x_k}\right) = C_D \frac{\mathcal{E}}{h} \left(\overline{\Theta'\Theta'}\right), \tag{3.22}$$

the model equation for the root-mean-square fluctuations of a passive scalar contaminant becomes

$$\bar{\mathcal{U}}_{\mathbf{k}} \frac{\partial (\Theta \Theta')}{\partial \mathcal{X}_{\mathbf{k}}} = 2C_{\mathbf{k}} \frac{\mathbf{k}}{\varepsilon} \left(\frac{\partial \bar{\Theta}}{\partial \mathcal{X}_{\mathbf{k}}}\right)^{2} - C_{\mathbf{k}} \frac{\varepsilon}{\mathbf{k}} \left(\Theta \Theta'\right) + C_{\mathbf{k}} \frac{\partial}{\partial \mathcal{X}_{\mathbf{k}}} \left(\frac{\mathbf{k}^{2}}{\varepsilon} \frac{\partial (\Theta \Theta')}{\partial \mathcal{X}_{\mathbf{k}}}\right). \tag{3.23}$$

Figures 2a and 2b present the complete model equations written for the plane and axisymmetric jets.

$$\hat{u}_{z} \frac{\partial \tau}{\partial z} + \hat{u}_{y} \frac{\partial \tau}{\partial y} = -C_{\tau_{1}} k \frac{\partial \hat{u}_{1}}{\partial y} - C_{\tau_{2}} \frac{\varepsilon T}{k} + C_{\tau} \frac{\partial}{\partial y} \left(\frac{k^{2}}{\varepsilon} \frac{\partial T}{\partial y} \right) \\
\hat{u}_{z} \frac{\partial k}{\partial z} + \hat{u}_{y} \frac{\partial k}{\partial y} = -T \frac{\partial \hat{u}_{z}}{\partial y} - \varepsilon + C_{k} \frac{\partial}{\partial y} \left(\frac{k^{2}}{\varepsilon} \frac{\partial k}{\partial y} \right) \\
\hat{u}_{z} \frac{\partial \varepsilon}{\partial z} + \hat{u}_{y} \frac{\partial \varepsilon}{\partial y} = -C_{\varepsilon_{1}} \frac{\varepsilon T}{k} \frac{\partial \hat{u}_{z}}{\partial y} - C_{\varepsilon_{2}} \frac{\varepsilon^{2}}{k} + C_{\varepsilon} \frac{\partial}{\partial y} \left(\frac{k^{2}}{\varepsilon} \frac{\partial \varepsilon}{\partial y} \right) \\
\hat{u}_{z} \frac{\partial \delta}{\partial z} + \hat{u}_{y} \frac{\partial \delta}{\partial y} = C_{\varepsilon_{3}} \frac{k^{2}}{k} \left(\frac{\partial \delta}{\partial y} \right)^{2} - C_{\varepsilon_{3}} \frac{\varepsilon}{k} \left(\frac{\partial \delta}{\partial y} \right) + C_{\varepsilon_{3}} \frac{\partial}{\partial y} \left(\frac{k^{2}}{\varepsilon} \frac{\partial \delta}{\partial y} \right) \\
\hat{u}_{z} \frac{\partial \delta}{\partial z} + \hat{u}_{y} \frac{\partial \delta}{\partial y} = 2C_{\varepsilon_{3}} \frac{k^{2}}{\varepsilon} \left(\frac{\partial \delta}{\partial y} \right)^{2} - C_{\varepsilon_{3}} \frac{\varepsilon}{k} \left(\frac{\partial \delta}{\partial y} \right) + C_{\varepsilon_{3}} \frac{\partial}{\partial y} \left(\frac{k^{2}}{\varepsilon} \frac{\partial \delta}{\partial y} \right)$$

Figure 2a. -- The model equations written for the plane jet.

$$\ddot{u}_{2} \frac{\partial T}{\partial z} + \ddot{u}_{r} \frac{\partial T}{\partial r} = -C_{r_{1}} k \frac{\partial \dot{u}_{2}}{\partial r} - C_{r_{2}} \frac{\partial T}{\partial r} + C_{r_{1}} \frac{\partial}{\partial r} \left(r \frac{k^{2}}{\epsilon} \frac{\partial T}{\partial r}\right)$$

$$\ddot{u}_{2} \frac{\partial k}{\partial z} + \ddot{u}_{r} \frac{\partial k}{\partial r} = -T \frac{\partial \ddot{u}_{2}}{\partial r} - E + C_{k} \frac{1}{r} \frac{\partial}{\partial r} \left(r \frac{k^{2}}{\epsilon} \frac{\partial k}{\partial r}\right)$$

$$\ddot{u}_{2} \frac{\partial E}{\partial z} + \ddot{u}_{r} \frac{\partial E}{\partial r} = -C_{E_{1}} \frac{\partial T}{\partial r} - C_{E_{2}} \frac{E^{2}}{k} + C_{E_{1}} \frac{\partial}{\partial r} \left(r \frac{k^{2}}{\epsilon} \frac{\partial E}{\partial r}\right)$$

$$\ddot{u}_{2} \frac{\partial E}{\partial z} + \ddot{u}_{r} \frac{\partial E}{\partial r} = C_{E_{1}} \frac{k^{2}}{k} \frac{\partial E}{\partial r} - C_{E_{2}} \frac{E^{2}}{k} \left(r \frac{k^{2}}{\epsilon} \frac{\partial E}{\partial r}\right)$$

$$\ddot{u}_{2} \frac{\partial E}{\partial z} + \ddot{u}_{r} \frac{\partial E}{\partial r} = C_{E_{1}} \frac{k^{2}}{k} \left(\frac{\partial E}{\partial r}\right)^{2} - C_{E_{2}} \frac{E}{k} \left(\overline{\partial e}\right) + C_{E_{1}} \frac{\partial}{\partial r} \left(r \frac{k^{2}}{\epsilon} \frac{\partial E}{\partial r}\right)$$

$$\ddot{u}_{2} \frac{\partial E}{\partial z} + \ddot{u}_{r} \frac{\partial E}{\partial r} = 2C_{e_{1}} \frac{k^{2}}{E} \left(\frac{\partial E}{\partial r}\right)^{2} - C_{e_{2}} \frac{E}{k} \left(\overline{\partial e}\right) + C_{e_{1}} \frac{\partial}{\partial r} \left(r \frac{k^{2}}{\epsilon} \frac{\partial E}{\partial r}\right)$$

$$\ddot{u}_{2} \frac{\partial E}{\partial z} + \ddot{u}_{r} \frac{\partial E}{\partial r} = 2C_{e_{1}} \frac{k^{2}}{E} \left(\frac{\partial E}{\partial r}\right)^{2} - C_{e_{2}} \frac{E}{k} \left(\overline{\partial e}\right) + C_{e_{1}} \frac{\partial}{\partial r} \left(r \frac{k^{2}}{\epsilon} \frac{\partial E}{\partial r}\right)$$

Figure 2b.--The model equations written for the axisymmetric jet.

IV. REDUCTION OF THE MODEL TO SIMILARITY FORM

In the self-preserving (similarity) region of the jet, each of the measurable flow characteristics is described by a scaling function evaluated along the axis and a function of the dimensionless distance, \(\bar{\chi}\), from the axis which is explicitly independent of axial position. With the proper scaling functions, the solution of the model equations in this region is simplified since the partial differential equations can be reduced to ordinary differential equations in the similarity variable \(\bar{\chi}\). In addition, the initial conditions at the nozzle exit of the jet do not influence the flow in the self-preserving region so only boundary conditions at the axis and the edge of the jet need specification.

The spreading rate of the jet, which is defined as the slope of the half-width, is shown in Figure 3 along with some of the other properties of the jet in the similarity region. The reduction of the model will be performed for the plane jet first and then for the axisymmetric jet.

To automatically satisfy the condition of continuity imposed by (2.2), the stream function, $\psi(z,y)$ is defined such that

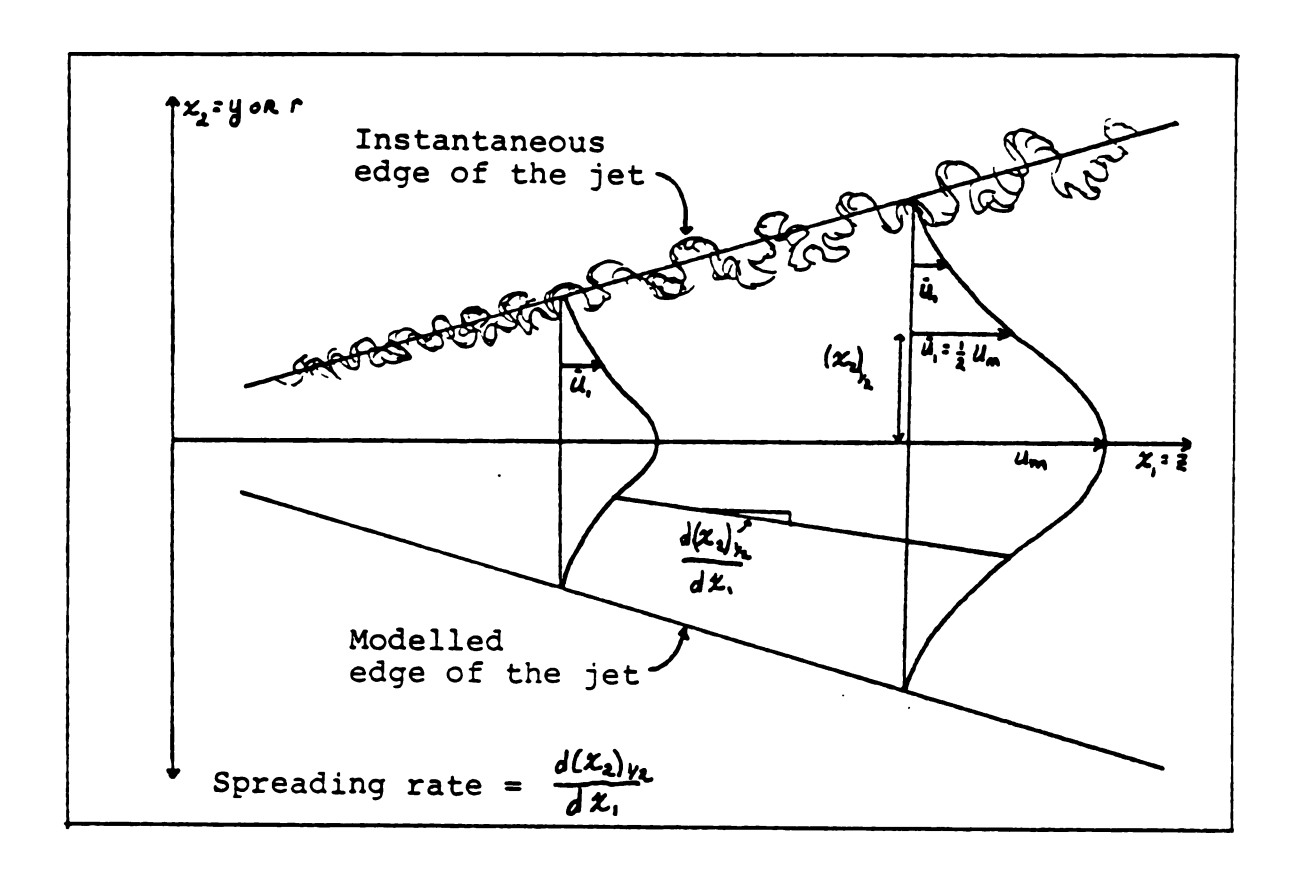


Figure 3.--Some properties of the axial jet in the region of similarity.

$$\psi_{,y} = \frac{\partial \psi}{\partial y} = \bar{\mathcal{U}}, \quad \text{and} \quad \psi_{,z} = \frac{\partial \psi}{\partial z} = -\bar{\mathcal{U}}_{2}. \quad (4.1)$$

Equation (3.1), neglecting the streamwise derivatives of the Reynolds stresses, can be written with the substitutions of (4.1) as

$$y, y, y = -y, y = -x,$$
 (4.2)

In the region of similarity,

$$\mathcal{Y} = \mathcal{U}_{m}(z) \, f(z)$$
 and $\mathcal{T} = \mathcal{U}_{m}^{2}(z) \, g(z)$ (4.3)

where χ = $\frac{1}{2}$ I(z) is the dimensionless distance from the axis, U_m is the velocity scale measured along the axis, and is the length scale of the jet as a function of axial position. Substitution of (4.3) into (4.2) yields

$$\left(\frac{\ell}{u_m}\frac{dU_m}{dz}\right)f'f' - \left(\frac{1}{u_m}\frac{d(u_m\ell)}{dz}\right)ff'' = -g' \tag{4.4}$$

where the primes now denote differentiation with respect to γ .

Because in the region of similarity the functions f and g cannot depend explicitly on either z or y, it is necessary that

$$\frac{1}{U_{m}}\frac{dU_{m}}{dz} = CONSTANT = \Omega, \quad \text{and} \quad \frac{1}{U_{m}}\frac{d(U_{m}R)}{dz} = CONSTANT = \Omega_{2}(4.5a,b)$$

It is noticed from (4.5b) that

$$\frac{1}{u_m} \frac{d(u_m l)}{d\bar{z}} = \frac{dl}{d\bar{z}} + \frac{l}{u_m} \frac{du_m}{d\bar{z}}.$$

Consequently, it is readily seen that the length scale must be linear in z, so

$$\ell(z) = \lambda_i(z-b) \tag{4.6}$$

where b is the virtual origin of the flow and λ_{r} is an unknown proportionality constant. In the self-preserving region, b«z, and will be left out of further considerations.

Using this result, the axial dependence of the velocity scale can be solved from (4.5a) as being

$$\frac{dU_m}{dz} = \frac{a_i}{\lambda_i} \frac{dz}{z} \qquad \text{or} \qquad U_m = A_i z^{n_i} \qquad (4.7a,b)$$

where A_1 is some constant and $n_1 = a_1/\lambda_1$. To evaluate the power n_1 , the conservation of the momentum flux across the width of the jet is employed. Thus,

$$gu_{0}^{2}d = \int (g\bar{u}_{1})\bar{u}_{1}dg = gu_{m}^{2}\int (f'(1))^{2}d1 = gA_{1}^{2}\lambda_{1}Z^{2n_{1}+1}\int (f'(1))^{2}d1 = CONSTANT.$$
 (4.8)

In order for (4.8) to be valid, it is readily seen that $n_1 = -\frac{1}{2}$ is required. Therefore,

$$U_{\mathbf{m}}(\mathbf{z}) = \mathbf{A}_{\mathbf{i}} \mathbf{z}. \tag{4.9}$$

Substitution of the above relations for the length and velocity scales into (4.4) yields the equation for the mean axial velocity in similarity form as

$$\frac{\lambda_i}{2} \left(f f' \right)' = g'. \tag{4.10}$$

Introducing the similarity forms for k and ϵ and using the previous forms for the mean velocities and γ ,

$$\bar{U}_{i} = U_{m}(z) f'(z) \tag{4.11a}$$

$$\bar{\mathcal{Q}}_{2} = -\lambda_{i} \mathcal{U}_{m} \ell^{*} \left(\frac{1}{2} f(\gamma) - \gamma f(\gamma) \right) \tag{4.11b}$$

$$T = \mathcal{U}_{m}^{1}(\frac{1}{2}) g(\gamma) \tag{4.11c}$$

$$k = U_m^2(2) \gamma(1) \tag{4.11d}$$

$$\mathcal{E} = \left(\mathcal{U}_{m}^{3}(\xi)/\chi(z) \right) m(\xi), \tag{4.12e}$$

the equations for \mathcal{T} , k, and ε for the plane jet can be reduced to their respective similarity forms as

$$-\lambda_{1}(fg + \frac{1}{2}fg') = -C_{T_{1}}Pf'' - C_{T_{2}}\frac{mg}{P} + C_{T}(\frac{P^{2}g'}{m})' \qquad (4.13a)$$

$$-\lambda_{i}(f'P + \frac{1}{2}fP') = -gf'' - m + C_{k}(\frac{P^{2}P'}{m})'$$
 (4.13b)

$$-\frac{\lambda_{1}}{2}\left(5f'_{m}+f_{m'}\right)=-C_{\epsilon_{1}}\frac{mg}{p}f''-C_{\epsilon_{2}}\frac{m^{2}}{p}+C_{\epsilon}\left(\frac{p^{2}m'}{m}\right)'. \quad (4.13c)$$

Equations (4.10) and (4.13 a, b, c) can be further reduced to a system of first order ordinary differential equations by making the following substitutions:

$$H = f' \tag{4.14a}$$

(4.14b)

$$t = C_k \frac{PT}{m} \tag{4.14c}$$

$$S = C_{\ell} \frac{P^{\ell} m'}{m}$$
 (4.14d)

The resulting system of nine first order differential equations required to solve the model for the uncontaminated jet are presented in Figure 4.

$$f' = H$$

$$g' = \frac{mR}{C_{\tau}P^{2}}$$

$$P' = \frac{mt}{C_{k}P^{2}}$$

$$m' = \frac{mS}{C_{\epsilon}P^{2}}$$

$$H' = \frac{2g'}{\lambda_{i}f} - \frac{H^{2}}{f}$$

$$R' = -\lambda_{i}(Hg + \frac{1}{2}fg') + C_{\tau_{i}}PH' + C_{\tau_{2}} \frac{mg}{P}$$

$$t' = -\lambda_{i}(HP + \frac{1}{2}fP') + gH' + m$$

$$S' = -\frac{\lambda_{i}}{2}(SHm + fm') + C_{\epsilon_{i}} \frac{mgH'}{P} + C_{\epsilon_{2}} \frac{m^{2}}{P}$$

$$\lambda'_{i} = O$$

Figure 4.--The similarity equations to be solved for the uncontaminated plane jet.

At the center of the jet, boundary conditions are imposed by symmetry,

$$\gamma = 0$$
, $t = S = g = f = 0$ and $H = 1$. (4.15a)

The remaining four boundary conditions are imposed at the edge of the jet $(y = \lambda_1 z)$. At this location both the mean velocity and the kinetic energy become zero. As a result, the dissipation of the kinetic energy is modelled as being controlled only by the turbulence structures within the jet, this term must also vanish at the edge of the jet. Thus,

at
$$\gamma = 1$$
, $P = m = H = t = 0$. (4.15b)

For the concentration profiles, the similarity forms are

$$\Theta = \Theta_{\mathbf{m}}(\mathbf{k}) \, \mathcal{G}(\mathbf{k}) \qquad \text{and} \qquad \overline{\Theta'\Theta'} = \Theta_{\mathbf{m}}^{2}(\mathbf{k}) \, \alpha(\mathbf{k}) \,, \qquad (4.16a,b)$$

where Θ_m is the scaling function for the concentration and is measured along the axis.

The model equation for the mean concentration is therefore written as

$$\lambda_i \left(\frac{2}{\Theta_m} \frac{d\Theta_m}{dz} \right) f'_g - \frac{1}{2} \lambda_i f'_g' = C_{\Theta} \left(\frac{P^i g'}{m} \right)'$$

so that for similarity to exist,

$$\frac{Z}{\Theta} \frac{d\Theta_m}{dZ} = CONSTANT = A_3$$
 and $\Theta_m = B_1 Z^3$ (4.17a,b)

To evaluate the power a_3 , the heat flux integral across the jet is investigated and reveals that

$$g = \frac{1}{2} \frac{1}{2}$$

Consequently, $a_3 = \frac{1}{2}$ is required, which is the same axial dependence displayed by the scaling velocity, and

$$\Theta_{m} = B_{i} z^{-\frac{1}{2}} \tag{4.19}$$

The similarity form of the equation for the mean contaminant concentration is written as

$$-\frac{\lambda_{i}}{2}\left(fq\right)' = C_{\Theta}\left(\frac{p^{2}q'}{m}\right)'. \tag{4.20}$$

With the above substitutions, the model equation for the root-mean-square concentration fluctuations can be written

$$-\lambda_{1}(f'\alpha + \frac{1}{2}f\alpha') = 2C_{0}\frac{p^{2}(q')^{2}}{m} - C_{0}\frac{m\alpha}{p} + C_{0}(\frac{p^{2}\alpha'}{m})'. \tag{4.21}$$

Equations (4.20) and (4.21) are reduced to a system of first order equations by the following substitutions:

$$\xi = C_0 \frac{P^2 Q^2}{m} \tag{4.22a}$$

$$S = C_0 \frac{P_{\alpha'}^2}{m}. \tag{4.22b}$$

The resulting system of four equations to be solved for the passive contaminant is presented in Figure 5. At the center of the jet, the value of the mean concentration is normalized and symmetry dictates that the derivative of the fluctuations be zero. Consequently,

at
$$\gamma = 0$$
, $g = 1$ and $g = 0$. (4.23a)

At the edge of the jet, both the mean and fluctuating concentrations are set to zero since molecular diffusion of the contaminant has been neglected from the model, so that

at
$$\gamma = 1$$
, $q = \alpha = 0$. (4.23b)

$$g' = \frac{m \, \S}{C_{\mathbf{q}_{1}} P^{2}}$$

$$\alpha' = \frac{m \, \S}{C_{\mathbf{q}_{1}} P^{2}}$$

$$\S' = -\frac{\lambda_{1}}{2} \left(Hq_{2} + f \, g' \right)$$

$$\S' = -\lambda_{1} \left(Hq_{2} + \frac{1}{2} f \, \alpha' \right) - 2 \, C_{\mathbf{q}_{1}} \frac{P^{2}(g')^{2}}{m} + C_{\mathbf{q}_{2}} \frac{m \, \alpha}{P}$$

Figure 5.--The additional similarity equations to be solved for the contaminated plane jet.

Since the variables describing the concentration of the passive contaminant do not appear in the equations for the uncontaminated jet, the two sets of equations are not coupled. Thus, the solution of the 7-k-& model for the uncontaminated jet may be obtained first and these results may be used to solve the equations for the contaminant later.

For the axisymmetric jet, the stream function is again defined such that the condition of continuity is

automatically satisfied with

$$\psi_{r} = \frac{\partial \Psi}{\partial r} = r \bar{U}_{z}$$
 and $\psi_{z} = \frac{\partial \Psi}{\partial z} = -r \bar{U}_{r}$, (4.24)

where r is the radial direction and z is again the axial direction. Equation (3.1), neglecting the streamwise derivatives of the Reynolds stresses, is written

$$\Gamma U_r \frac{\partial U_z}{\partial r} + \Gamma U_z \frac{\partial U_z}{\partial \overline{z}} = -\frac{\partial}{\partial r} (\Gamma \overline{I}). \tag{4.25}$$

In the region of similarity,

$$\Psi \in \mathcal{U}_{m}(z)$$
 $f(z)$ and $\gamma = \mathcal{U}_{m}^{2}(z)$ $g(z)$ (4.26a,b)

where $\gamma^2 / \gamma_{(2)}$. Substitution of (4.26a,b) into (4.25) results in

$$\frac{1}{u_{m}l} \frac{d(u_{m}l^{2})}{dz} \left(\frac{ff}{2}\right)' - \frac{dl}{dz} \left(f'f'\right)' - \frac{1}{u_{m}^{2}} \frac{d(u_{m}^{2}l)}{dz} \left(\frac{f'f'}{2}\right)' - \frac{dl}{dz} \lambda \left(\frac{f'f'}{2}\right)' = (\lambda g)'$$
(4.27)

This indicates that again,

where, as in the case of the plane jet, the effect of the virtual origin on has been deleted.

Substitution of (4.28) into the first term of (4.27) leads to

$$U_{\mathbf{m}} = A_{\mathbf{z}} \mathbf{z}^{\mathbf{n}_{\mathbf{z}}}, \tag{4.29a}$$

as in the case of the plane jet. The power n_2 is again obtained from the momentum flux integral corresponding to (4.8) and shows that $n_2 = -1$ for the similarity region of the axisymmetric jet. Thus,

$$U_{m}(z) = \theta_{z} z^{-1} \tag{4.30}$$

Using the similarity forms

$$U_{r} = \lambda_{r} U_{r} f^{2} \left(f'(\gamma) - \frac{1}{\gamma} f'(\gamma) \right) \tag{4.31a}$$

$$U_2 = U_n(z) \frac{1}{\lambda} f'(\gamma) \qquad (4.32b)$$

and the previous expressions for \mathcal{T} , k, \mathcal{E} , $\dot{\Theta}$, and $\dot{\Theta}$ used in the case of the plane jet, the model equations for \mathcal{T} , k, and \mathcal{E} for the axisymmetric jet can be respectively reduced to

$$-\lambda_{i}(2f'g+fg') = -C_{ri}P(f''-\frac{f'}{i}) - C_{ri} \frac{mg}{P} + C_{r}(\frac{p^{2}g'}{m})'$$
 (4.33a)

$$-\lambda_{i}(2f_{i}^{2}+f_{i}^{2})=-g(f_{i}^{2}-\frac{f_{i}^{2}}{2})-\chi_{i}^{2}+C_{k}(\chi_{i}^{\frac{2}{m}})'$$
(4.33b)

$$-\lambda_{1}(4f'm+fm')=-C_{1}\frac{mg}{p}(f''-f')-C_{2}(\frac{m^{2}}{p}+C_{2}(\frac{p^{2}m'}{m})')$$
 (4.33c)

This system is also reduced to a first order system by making the following substitutions:

$$H = \frac{f}{2} \tag{4.34a}$$

$$\mathcal{R} = C_T \frac{P^2 g'}{m} \tag{4.34b}$$

$$t = C_k \frac{p^2 p'}{m} \tag{4.34c}$$

$$S = C_E \frac{P^L m'}{m}$$
 (4.34d)

The resulting system of equations to be solved for the axisymmetric jet is presented in Figure 6 and is subject to the same boundary conditions described for the plane jet.

$$f' = \frac{1}{2}H$$

$$g' = \frac{m^{2}}{C_{1}P^{2}}$$

$$P' = \frac{m^{4}}{C_{1}P^{2}}$$

$$m' = \frac{m^{4}}{M^{4}}(\lambda g' + g) - \frac{1}{2}H^{2}f$$

$$R' = -\frac{\lambda}{A^{4}}(\lambda g' + g') + C_{12}\frac{mg}{P} + C_{11}PH' - \frac{R}{A^{4}}$$

$$E' = -\frac{\lambda}{A^{4}}(\lambda g' + g') + m + gH' - \frac{1}{2}A$$

$$E' = -\frac{\lambda}{A^{4}}(\lambda g' + g' + g') + m + gH' - \frac{1}{2}A$$

$$S' = -\frac{\lambda}{A^{4}}(A_{1}Hm + fm') + C_{22}\frac{m^{2}}{P} + C_{21}\frac{mg}{P}H' - \frac{1}{2}A$$

$$\lambda'_{1} = 0$$

Figure 6.--The similarity equations to be solved for the uncontaminated axisymmetric jet.

With the similarity forms mentioned above, the model equation for the mean concentration of the passive contaminant reduces to

$$-\lambda_{i}fg'+\left(\frac{1}{G_{m}}\frac{d\Theta_{m}}{dz}\right)f'g=C_{\Theta}\left(\gamma\frac{P^{2}g'}{m}\right)'$$
(4.35)

from which it is seen that again the scaling function takes the form

^{*}The term 2 \gamma\] is not used in the calculations because of a singularity in it at \gamma=0. [c.f. Rotta (1975)]

$$\Theta_{m} = \mathcal{B}_{2} \tilde{z}. \tag{4.36}$$

As before, the constant a_4 is obtained by examining the heat flux integral corresponding to equation (4.18) and results in

$$\Theta_{n}(z) = B_{2} z^{-1} \tag{4.37}$$

Making this substitution in (4.35) gives the similarity form of the equation for the mean contaminant concentration as

$$-\lambda_{i}(fg) = C_{\theta}(\sqrt{\frac{p^{2}g'}{m}}). \tag{4.38}$$

The similarity form of the equation for the rootmean-square of the concentration fluctuations can now be immediately written as

$$-\lambda_{1}\left(2f'\alpha+f\alpha'\right)=2C_{\theta_{1}}\sqrt{\frac{p^{2}(g')^{2}}{m}}-C_{\theta_{2}}\sqrt{\frac{m\alpha}{p}}+C_{\theta_{1}}\left(\sqrt{\frac{p^{2}\alpha'}{m}}\right). \tag{4.39}$$

Equations (4.38) and (4.39) are also reduced to a system of first order equations by the substitutions of (4.22a,b). The resulting system of four equations to be solved for the passive contaminant is presented in Figure 7.

The boundary conditions employed differ slightly from those in the case of the plane jet because of difficulties encountered in the calculations. The previous condition that the mean concentration be zero at the

edge of the jet is replaced by a symmetry condition of the mean concentration at the axis of the jet. The resulting boundary conditions are thus

$$\gamma = 0$$
, $\beta = \beta = 0$ and $\beta = 1$ (4.40a)
 $\gamma = 1$, $\alpha = 0$. (4.40b)

$$g' = \frac{m}{C_{a_1}P^{\lambda}}$$

$$\alpha' = \frac{m}{C_{a_1}P^{\lambda}}$$

$$g'_{2} - \frac{\lambda}{\lambda}(Hg + fg') - \frac{g}{\lambda}$$

$$g' = -\frac{\lambda}{\lambda}(2H\alpha + f\alpha') - 2C_{a_1}\frac{P^{\lambda}(g')^{\lambda}}{m} + C_{b_2}\frac{m\alpha}{P} - \frac{g}{\lambda}$$

Figure 7.—The additional similarity equations to be solved for the contaminated axisymmetric jet.

An analytic form for the mean passive contaminant concentration is obtainable from equation (4.38) for the axisymmetric jet and from (4.20) for the plane jet. However, the resulting expression contains an integral that must be calculated numerically. Consequently, the profile is calculated from the differential equations already described.

The numerical scheme used to perform the calculations was developed by Wood, based on Keller's (1974) box scheme with Newton iterations. The algorithm is designed to solve systems of non-linear first order ordinary

differential equations associated with two-point boundary value problems.

V. RESULTS AND DISCUSSION

In the measurements of the physical characteristics of a free turbulent jet, the most easily made and consistent measurement is that of the spreading rate of the jet. It is also found that the calculated spreading rate is quite sensitive to the set of constants employed in the model. Thus, the comparison of the calculated spreading rate to the data is used here as the primary test of the model. The other major comparison between the calculated results and the reported data is the value of the turbulence kinetic energy at the jet axis. This provides a basis for determining the ability of the model to predict the magnitude of the turbulence intensity relative to the mean velocity, although the reported data is less consistent [Wood (1978)] for this value than for the spreading rate.

The sensitivity of the spreading rate in the axisymmetric jet on the constants \mathcal{C}_{0} , \mathcal{C}_{k} , and $\mathcal{C}_{\ell 2}$ was investigated and the results are presented in Table 1. It is seen that of these three, the spreading rate is the most sensitive to changes in $\mathcal{C}_{\ell 2}$. The percentage change in the spreading rate is almost six times as great as the change in $\mathcal{C}_{\ell 2}$.

TABLE 1.--Sensitivity of the spreading rate on \mathcal{C}_{rr} , \mathcal{C}_k , and $\mathcal{C}_{\ell k}$.

% Change in	Spreading Rate	28	-5	23
	Cer			4
% Change in	C.		15	
	<i>G</i> 21	29		

TABLE 2. -- Sets of constants evaluated.

								Spread	Spreading Rate
Author (8)	$C_{\mathbf{r}_{i}}$	Cri	Cr	C.	Ce,	Ces	CE	Plane Jet	metric Jet*
Hamjalic & Launder# (197)	961.	2.80	80.	.07	.07 1.45	2.00(1.90)	90.	.085	.103
Rodi [#] (1972)	.252	2.80	.10	60.	1.45	2.00(1.925)	.082	.082 117	.125
Launder, Reece, & Rodi (197)	.190	1.50	.11	60.	1.44	1.90(1.85)	080.	.123	.146
Wood (1978)	.135	1.50	.10	.10	.10 1.45	1.90(1.85)	.082	.082 .088	.104

Because the calculated spreading rate is greater for the axisymmetric jet than the plane jet and the opposite occurs in the experimental data, the spreading rate is severely over-estimated in the axisymmetric jet when the same set of constants is utilized for both geometries. As a result, several empirical modifications to the constants have been suggested [c.f. Pope (1978)] to better predict the spreading rate in the axisymmetric jet. The suggestion by Launder et. al. (1972) that

$$C_{E2} = C_{E2} - .0667 \left\{ \frac{\varkappa_{u_m}}{2U_m} \left(\left| \frac{dU_m}{dz} \right| - \frac{dU_m}{dz} \right) \right\}^{0.2}$$
 (5.1)

is used here for the axisymmetric jet. Modifications to \mathcal{C}_{ℓ} presented by Pope (1978) were not investigated because of the strong agreement between the authors listed in Table 2 on its value.

Table 2 lists the sets of constants evaluated and the resulting spreading rates for the plane and axisymmetric jets, with the modification of \mathcal{C}_{Ω} given in parentheses. From Table 2, it is seen that the set of constants proposed by Wood (1978) give the best overall agreement with the spreading rates from the experimental data of .11 for the plane jet and .087 for the axisymmetric jet [Launder and Morse (1977)]. These constants were used in the remaining calculations and the results are presented in Figures 8 through 12.

The constants employed in the evaluation of the passive contaminant properties are listed in Table 3. The value of $C_{\bullet g}$ is adopted directly from Chen and Rodi (1975). The diffusion coefficient for the contaminant fluctuations is modelled as the ratio of the eddy viscosity to a turbulent Prandtl-Schmidt number. For the eddy viscosity fitting the form of equation (2.3), the coefficient C_{μ} is typically assigned a value of .09. The Prandtl-Schmidt number for plane and axisymmetric jets has been reported by Launder (1976) and Spalding (1971) to be .9 and .7, respectively, thereby accounting for the two values for $C_{\bullet g}$ given in Table 3.

Although the model predicts that C_{\bullet} be multiplied by a factor of two, the actual multiplying factor used in the calculations is 1.6 so that a value of .133 is reported here for C_{\bullet} instead of the same value as C_{\bullet} . Chen and Rodi report a value for C_{\bullet} as 1.25. However, from Launder (1976) this value corresponds to bouyant flows, and a value as high as 2.0 for C_{\bullet} is reported. Thus, the value 1.7 for C_{\bullet} is used here as an intermediate between these two extremes. No attempt beyond this has been made here to obtain an optimum set of constants to best fit the available data.

Figure 8 presents the profiles of the mean axial velocity and the mean contaminant concentration versus the similarity variable, γ , across the plane jet. The

TABLE 3.--Constants used in the model equations for the passive contaminant properties

C••	C.	Ca	Con
.165	.1 (.129)	.133	1.7

profiles of the turbulence kinetic energy and the square of the root-mean-square contaminant concentration fluctuations for the plane jet are presented in Figure 9. Figures 10 and 11 give the corresponding results for the axisymmetric jet.

In Figure 9, it is noticed that the kinetic energy of the turbulence exhibits a maximum some distance from the axis of the jet. The location of the maximum corresponds quite well with the data of Bradbury (1965). Since the kinetic energy is produced from the mean shear rate, $\partial L/\partial z_1$, it is expected that the maximum kinetic energy should occur near the location of maximum production of energy. Comparison of Figures 8 and 9 shows that this is the case here. Although the value of the maximum kinetic energy is under-estimated, the value relative to the value at the axis is in close agreement with the data.

The profile for the kinetic energy in the axisymmetric jet presented in Figure 11 does not agree with the data of Wygnanski and Fiedler (1969) nearly as well as

for the plane jet. This is not entirely unexpected since the mean velocity profile in Figure 10 is significantly over-estimated by the model. Even though the predicted profile of the kinetic energy is wider than the data, the lack of a maximum energy away from the axis is in agreement with the experimental measurements. The value of the kinetic energy at the axis is again underestimated but the proportional increase over the same value for the plane jet is comparable to that of the data.

The predicted mean contaminant concentration profiles presented in Figures 8 and 10 are wider than the mean axial velocity profiles for both geometries, which is consistent with the experimental data. However, the curves do not exhibit the inflections in the outer regions of the jets that are evident in the data of Bashir (1973) and Becker, Hottel, and Williams (1976), respectively. The most likely reason for this behavior is that in an actual jet, the flow is largely intermittent between high turbulence levels and ambient conditions in the outer region. The model employed here assumes a sharp interface between a fully turbulent jet flow and a stationary ambient. Since the turbulence induced fluxes of contaminant concentration are much greater than molecular diffusion fluxes, the predicted profile is expected to be greater than the actual profile.

In Figure 9, the square of the root-mean-square contaminant fluctuations is presented along with the data of Bashir (1973). The predicted profile agrees well with the data in the central region of the jet but is underestimated near the axis and the edge of the jet. The predicted value of .032 at the axis is significantly less than Bashir's .052, although no other data was found to compare either profile with. The set of constants used in the model were not varied either so that an optimization of the constants may lead to better agreement.

The normalized contaminant fluctuations in the axisymmetric jet are presented in Figure 12 with the data of Becker, Hottel, and Williams (1967). As with the mean contaminant concentration profile, the inflection exhibited by the data is not present in the calculated profile. The explanation offered for this is the same as in the previous case. The over-prediction of the profile may also be partially attributable to the over-prediction of the mean velocity. Chen and Rodi (1975) present the results of their calculations for the same quantity and report a value at the axis of about 0.16 whereas this study estimates the corresponding value as 0.045. Again, an optimization of the constants may lead to a better agreement between these two values.

Since it is hoped that this model can serve as a precurser to modelling efforts of two-phase flows,

numerical results as accurate as possible are desired. Consequently, the desire to obtain a single set of constants to be universally used to describe all free shear flows may justifiably be over-ridden by the need to obtain more accurate results for a particular flow and geometry. The empirical modification of $\mathcal{C}_{\mathfrak{L}2}$ suggested by Launder et. al. (1972) adopted here is an example of this. Since the universality of the constants is already lost through the use of this modification, further adjustments to the constants to better approximate the experimental data are seen as justifiable.

The model has shown that it can adequately describe the characteristics of the free turbulent jet and the agreement between the calculated results and the reported data may be improved by adjusting the constants for the specific geometry in question. Thus, further inquiry into two-phase jets based on this model is considered to be acceptable.

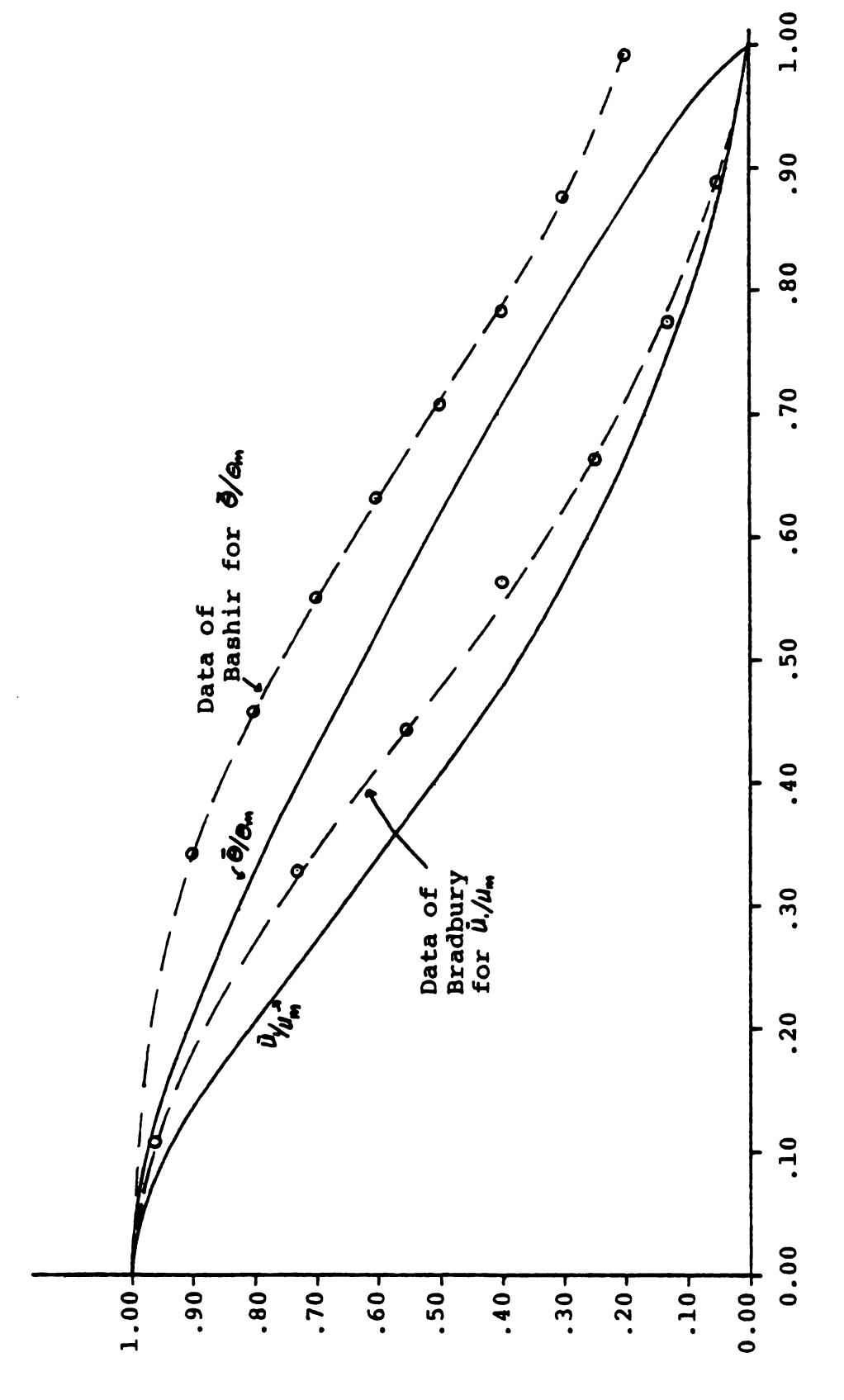


Figure 8.--Comparison of predictions of the mean axial velocity and mean contaminant concentration profiles in the plane jet with experimental data.

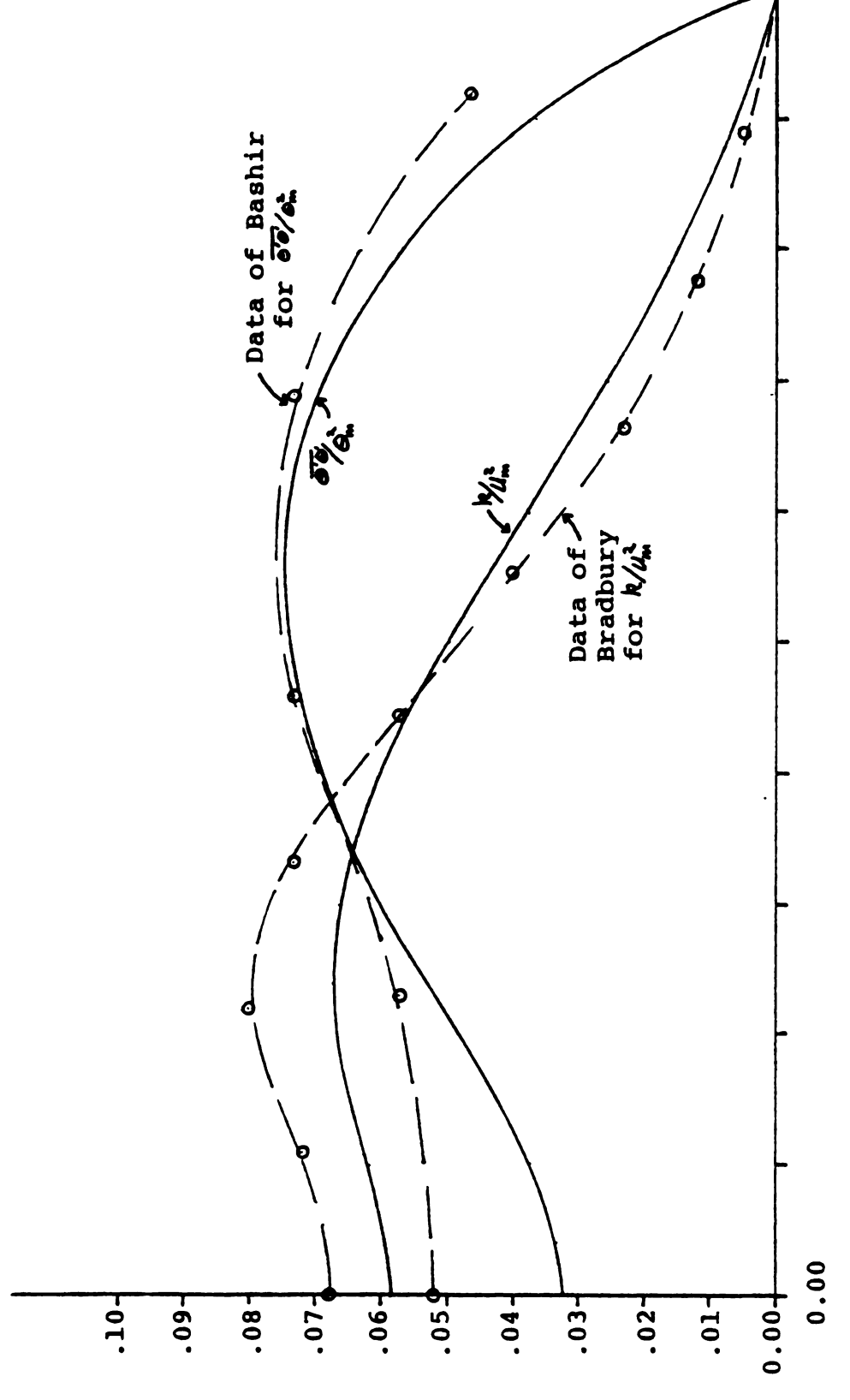


Figure 9. -- Comparison of predictions of the turbulence kinetic energy and the square of the root mean square contaminant concentration fluctuations in the plane jet with experimental data.

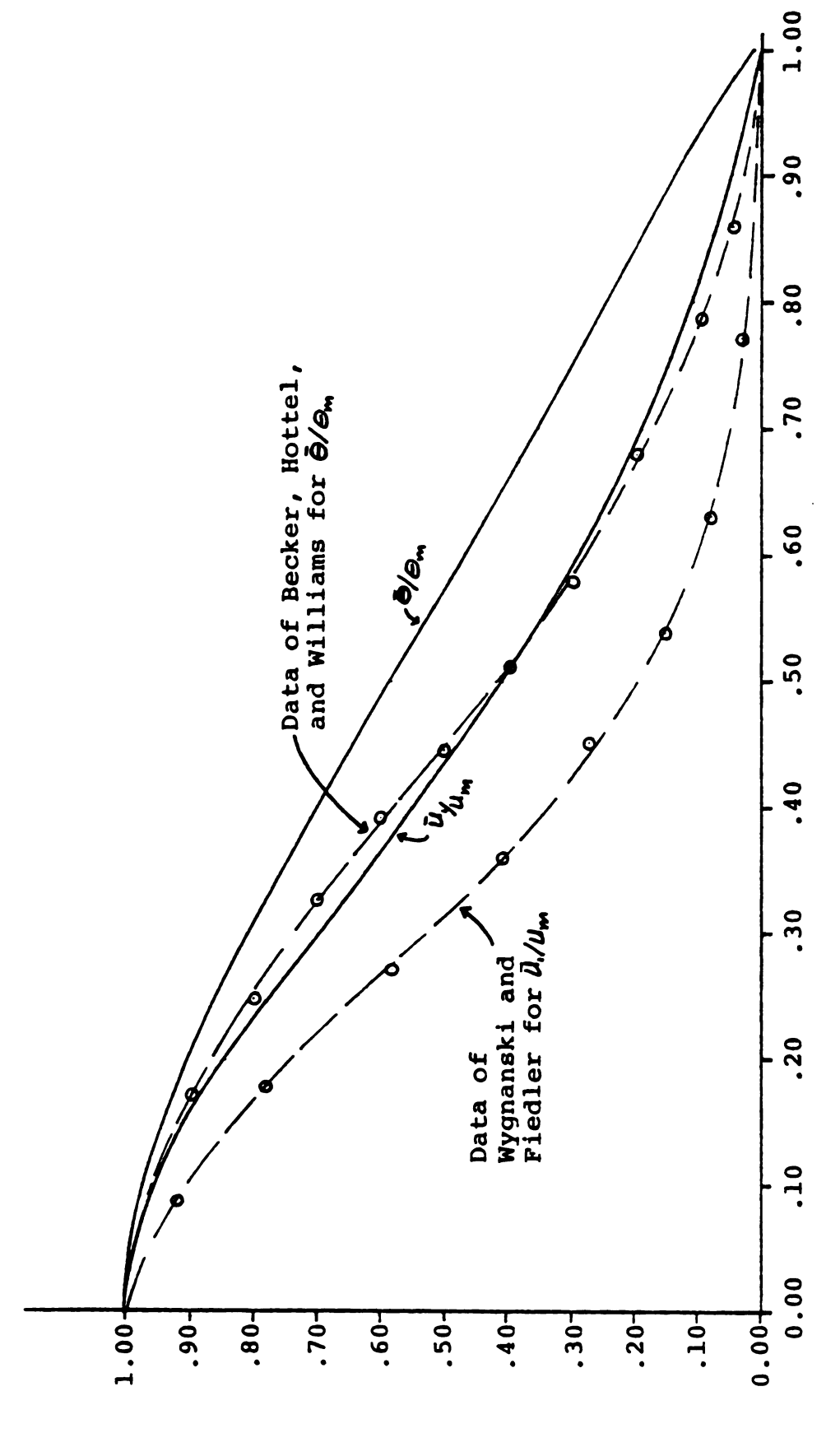


Figure 10.--Comparison of predictions of the mean axial velocity and mean contaminant concentration profiles in the axisymmetric jet with experimental data.

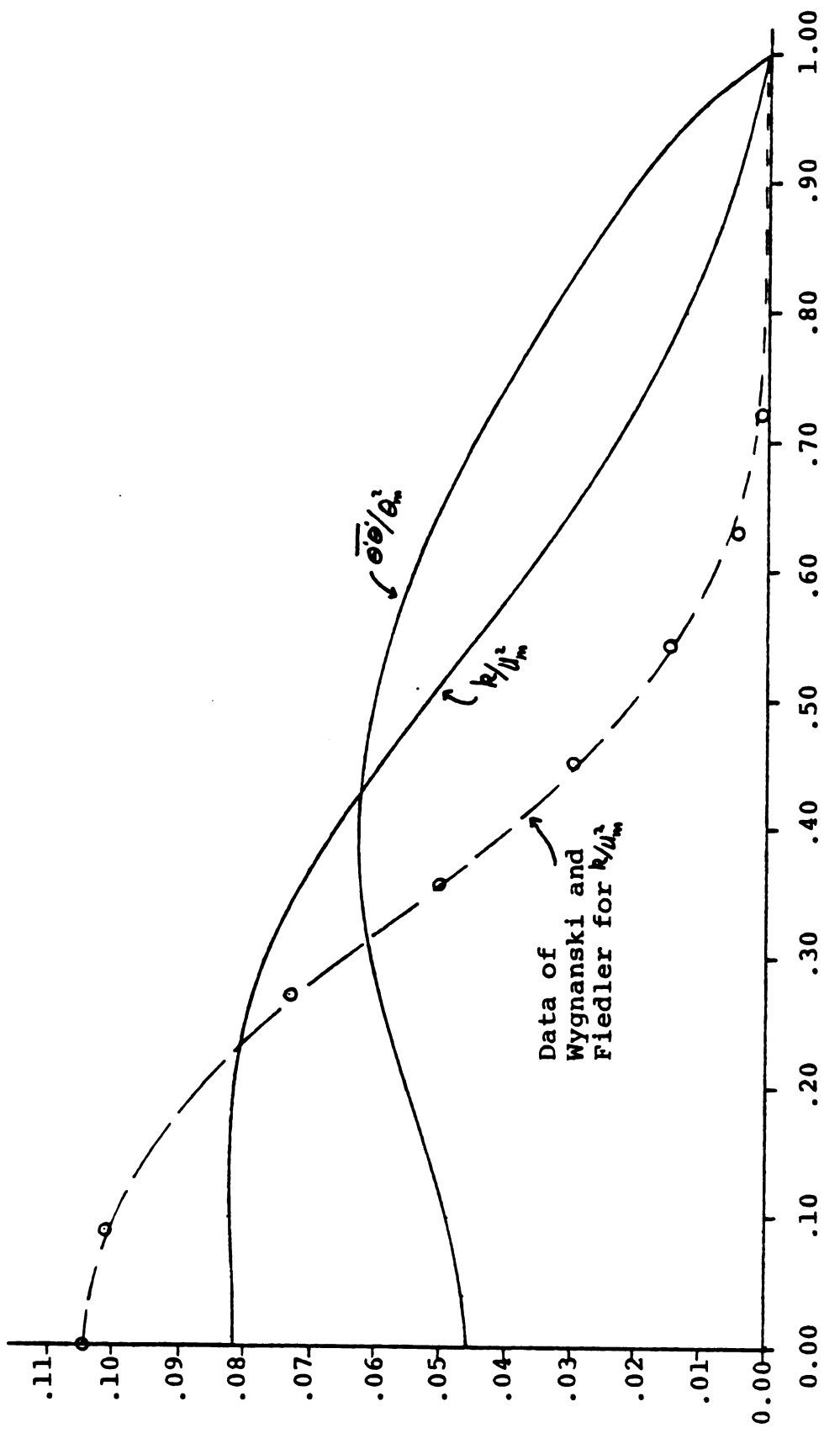


Figure 11.--Comparison of the prediction of the turbulence kinetic energy with experimental data and the prediction of the square of the root mean square contaminant concentration fluctuations in the axisymmetric set.

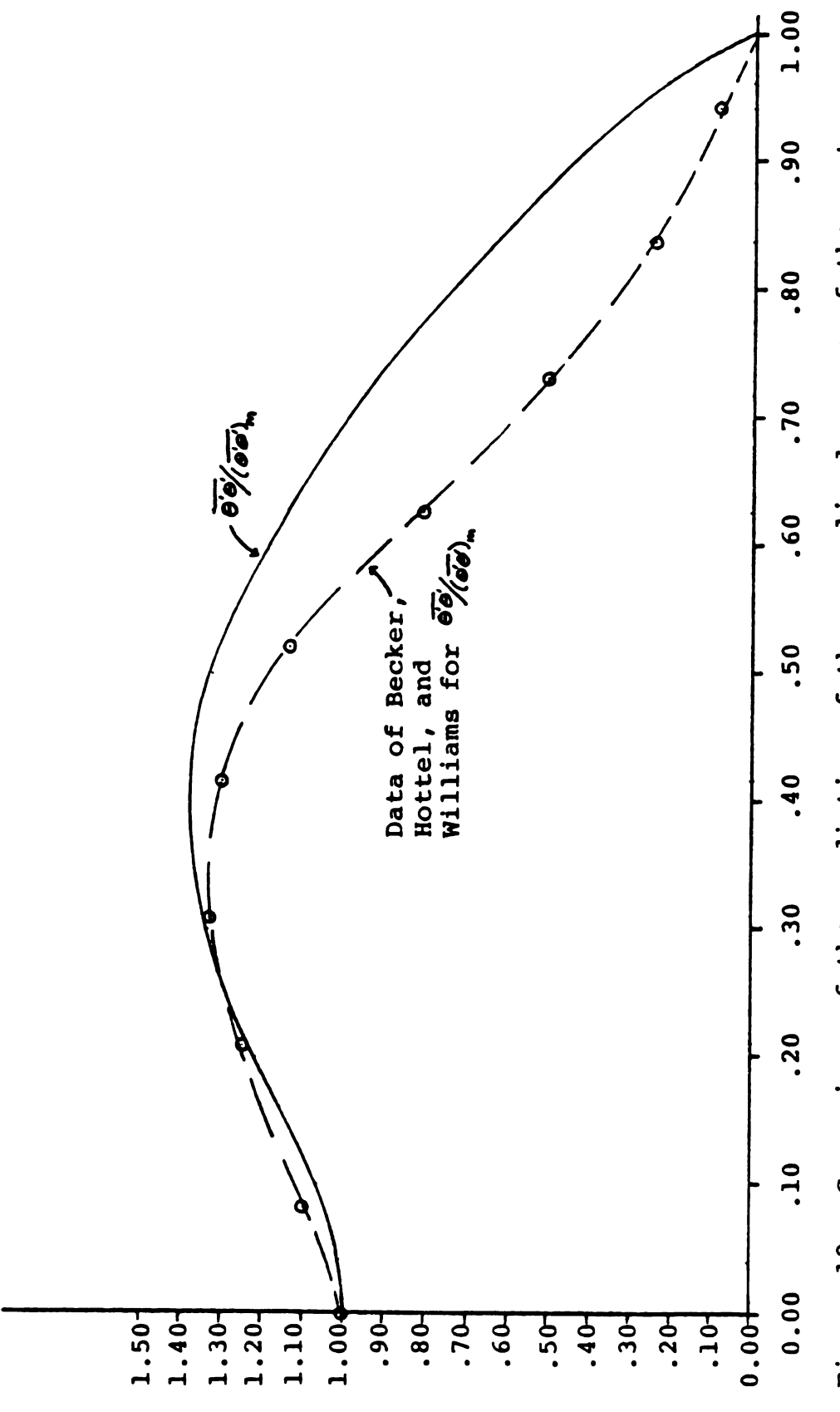


Figure 12.--Comparison of the prediction of the normalized square of the root mean square contaminant concentration fluctuations in the axisymmetric jet with experimental data.

VI. TWO-PHASE JETS

The description of two-phase jets is inherently more complicated than that of single-phase jets. One major contribution to this is the strong coupling of the heat and momentum transport processes between the phases which can significantly alter the structure of the flow, especially for the case of high concentrations of relatively large, heavy particles.

In the modelling efforts of two-phase flows, two approaches are commonly used. One method involves considering the fluid-particle suspension as a single inhomogeneous continuum. The internal stresses arising from interactive forces between the phases are described by constitutive equations in terms of the bulk variables. The other approach, which is used here, is to consider the suspension as two separate continua that interact with each other through explicit body forces. This requires the use of a continuum hypothesis for the particulate phase which is strictly valid only under the restrictions of relatively dense suspensions of fine particles [Hinze (1972)]. Even when these restrictions are not fully satisfied, the procedure often followed is to assume the validity of the hypothesis and compare

the results of the calculations with experimental data to check the assumption.

In this section, some general characteristics of two-phase jets are discussed along with some requirements of modelling schemes. The model equations applicable to two-phase jets are also looked at and some modelling efforts of the interaction terms [c.f. Damon et. al. (1977), Melville and Bray (1979a,b)] are examined. In addition, some of the specific physical characteristics of two-phase jets and their differences from single-phase jets are discussed.

In the results of the calculations of the profile of a passive scalar contaminant concentration, it was found that the profile of the scalar across the jet is significantly wider than the profile of the axial velocity. However, when the transition is made from passive scalar to discrete particulate contaminants, the opposite trend occurs; that is, the particles' profile is narrower than the velocity profile. Danon et. al. (1977) found that as the particle loading increased, the width of the jet decreased which is taken as an indication of a reduction in the turbulence level within the jet. Melville and Bray (1979a) have indicated that the effect of the particle loading on the fluid may become significant in the mass, momentum, and energy balances in the primary (fluid) phase. This effect is made clear in the work of

Laats and Frishman (1970) in which they found that neither the velocity nor the particulate profile attained a self-preserving form in heavily loaded jets. When sufficiently light loadings are used, Melville and Bray (1979a) have reported that all of the particle mass flux profiles attained a self-preserving form.

(1979b) assert that the particle transport may be described by a dependence of the turbulent Schmidt number, which is the ratio of the turbulent momentum and mass diffusivities, on the particle loading and flow characteristics. The dependence is restricted by the requirement that the Schmidt number decays to that of an uncontaminated jet as the particle loading tends toward zero. Abramovich and Girshovich (1973) propose that the dependence on particle loading is linear for the case of finely divided particles that are totally entrained by the fluid. They also assert that the Schmidt number increases toward infinity as the coarseness of the particles is increased.

Assuming that the previously discussed continuum hypothesis applies, the following equations of continuity for the two phases may be written [Danon et. al. (1977)] as

$$\frac{\partial}{\partial t}(1-\phi) + \frac{\partial}{\partial x_{i}}((1-\phi)u_{i}) = 0 \tag{6.1}$$

and
$$\frac{\partial}{\partial t}(\phi) + \frac{\partial}{\partial x_j}(\phi u_{pj}) = 0.$$
 (6.2)

Here, ϕ represents the volume fraction of the particulate phase, which is much less than unity, and \mathcal{U}_{j} and \mathcal{U}_{j} are the \mathcal{Z}_{j} -direction components of the fluid phase and particulate phase velocities, respectively.

The conservation of momentum in the fluid phase may be expressed as

$$\frac{\partial}{\partial t}((1-\phi)u_i) + \frac{\partial}{\partial x_i}((1-\phi)u_iu_i) = -\frac{1}{9}\frac{\partial P}{\partial x_i} + \nu \frac{\partial^2 u_i}{\partial x_i \partial x_i} + \frac{1}{9}F_i$$
 (6.3)

where F_i , the body force term arising from interactions between the two phases, has been described [Danon et. al. (1977), Melville and Bray (1979b)] by Stokes law as

$$F_{i} = \frac{18\mu}{d^{2}} \phi(u_{pi} - u_{i}). \tag{6.4}$$

Since it is found that the mean velocities of the two phases are virtually equal in the region of similarity [c.f. Danon et. al. (1977), Melville and Bray (1979b)], an additional equation for the momentum in the particulate phase is not required. Fenton and Stukel (1976), however, in their study of a two-phase, two-dimensional wake, employed an equation for the momentum of the particulate phase.

Noting that $\vec{\phi} \ll |$, $\vec{U}_{\vec{p}j} = \vec{U}_{j}$, and time-averaging, equations (6.1), (6.2), and (6.3) may be re-written as

$$\frac{\partial}{\partial z_i}(\bar{u}_i) = 0, \tag{6.5}$$

$$\frac{\partial}{\partial z_{i}} \left(\bar{\phi} \bar{u}_{i} \right) = \frac{\partial}{\partial z_{i}} \left(-\bar{\phi}' u_{i}' \right), \tag{6.6}$$

and
$$\bar{\mathcal{U}}_{ij} \frac{\partial \bar{\mathcal{U}}_{i}}{\partial z_{ij}} = \frac{\partial}{\partial z_{ij}} \left(-\bar{\mathcal{U}}_{i}' \mathcal{U}_{ij}' \right) + \frac{18\nu}{d^{2}} \bar{\mathcal{O}}' \left(\mathcal{U}_{Fi}' - \mathcal{U}_{i}' \right),$$
 (6.7)

respectively, for high Reynolds numbers. For light loadings, the resulting force term in (6.7) is seen to be negligible. Thus, there is only an insignificant effect on the momentum profile across the jet as a result of interactions between the two phases.

The turbulence kinetic energy equation for the fluid phase may be obtained from equation (6.3) in the same manner as in the single-phase jet. The resulting equation is the same as (3.11) with the exception that the term

$$\frac{18\nu}{d^{2}} \left[(\vec{u}_{p_{i}} - \vec{u}_{i}) \vec{u}_{i} \phi' + (\vec{u}_{p_{i}} - u_{i}') \vec{u}_{i}' \phi' + (\vec{u}_{p_{i}} - u_{i}') \vec{u}_{i}' \phi' \right]$$
 (6.8a)

is added to the R.H.S. of (3.11) in the two-phase model equation. The first term in (6.8a) is approximately zero by the approximate equality of the mean velocities and the third term is considered to be negligible relative to the second because it is third order in the velocity fluctuations. Thus, the remaining additional term to (3.11) is

$$\frac{18\nu}{d^2} \left(\overline{U'_{ii} - U'_{i}} \right) U'_{i} \quad \overline{\phi} \tag{6.8b}$$

and is referred to as the "added dissipation."

In order to obtain a solution to the kinetic energy equation, it is necessary to model the correlation. This is accomplished by observing that

$$2k \ge -(\overline{U_{Pi}^{\prime} - U_{i}^{\prime}})U_{i}^{\prime} \ge 0, \tag{6.9}$$

where the upper bound represents the case when the particles are stationary with respect to the turbulent fluid fluctuations and the lower bound corresponds to the case where the particles exactly follow the turbulent fluid fluctuations. Danon et. al. (1977) have proposed that this correlation be modelled as

$$-(u_{i}^{*}-u_{i}^{*})u_{i}^{*}=2k(1-exp[-B\dot{c}_{7}/\dot{c}_{e}]) \qquad (6.10)$$

where B is an empirical constant, tp is the particle response time scale, and te is the time scale of the smallest eddies given by

$$t_{p} = \frac{P_{p} d^{2}}{\mu} = \frac{P_{s} \phi d^{2}}{\mu} \quad \text{and} \quad t_{e} = \left(\frac{\nu}{\epsilon}\right)^{k_{z}}. \tag{6.11}$$

This model is seen to satisfy the upper and lower bounds of (6.9) when the ratio tp/te tends toward infinity and zero, respectively, although no justification for the exponential form has been offered.

For sufficiently small values of tp/te, (6.10) can be linearized by a Taylor series expansion of the exponential to

$$-(\overline{u_{i}^{*}-u_{i}^{*}})u_{i}^{*}=2k(8^{t}\%_{e})=2kB\beta_{s}\frac{d^{2}}{(\mu\rho)^{1/2}}\sqrt{2}^{2}$$
(6.12)

which is linear in particle loading and agrees with the result of Owen (1969).

When the linearized model of (6.12) is attempted to be cast into a similarity form, it is found that the dependence on axial position of this term is not compatible with the rest of the terms in the kinetic energy equation. The same behavior is exhibited by the added terms to the turbulence shear stress and energy dissipation equations. Consequently, another method of solving the model equations is required to calculate the profiles across the two-phase jet.

From the experimental work of Laats and Frishman (1970), information can be obtained concerning the effects of particle size and initial loading on the spreading rate and mean velocity distributions as well as on the turbulence structure within the two-phase jet. For values of \mathcal{K}_o , the initial mass ratio of the particulate phase to the fluid phase, between 0.0 and 0.05, the fluid velocity distribution at the nozzle exit is about the same as in the turbulent region further downstream with

Uom $\mathcal{N}^{\sim}1.25$. The subscript om indicates the maximum value at the nozzle exit and the superscript denotes the average value at the nozzle exit. However, upon further increasing the initial loading to $\mathcal{K}_{\sim}0.7$, the fluid velocity distribution becomes almost uniform $(\frac{\mathcal{N}_{\sim}}{\mathcal{N}^{\circ}}\sim1.0)$ at the nozzle exit. The initial velocity distribution of the particulate phase exhibits the opposite trend, with the distribution becoming more non-uniform with increasing \mathcal{K}_{o} for a given particle size as well as with increasing particle size for a given \mathcal{K}_{o} .

The data also reveals that the particle mass flux g(kg particles/m²sec) attains a self-preserving form for %~1.0 whereas the mean axial fluid velocity profile fails to become similar. Although absolute similarity does not occur for the mean fluid velocity, the deviation from self-preservation is not large and is readily evident only for fine particles. Consequently, the experimenters concluded that the velocity profile may be considered to be similar over discrete segments of %D without significant error.

Division of the relative particle mass flux, g/gm, by the relative velocity, U/Um, gives the relative concentration of the particles, K/Km, providing that the difference between the mean velocity of the two phases may be neglected. Thus,

$$\frac{\chi}{\chi_m} = \frac{3/\beta_m}{u/u_m} = \frac{f_1(r/r,s_2)}{f_2(r/r,s_u)},$$
(6.13)

taking the velocity profile to be of a self-preserving form. The values $f_{.s_0}$ and $f_{.s_u}$ denote the distance from the axis where the particle mass flux and axial velocity are half of their respective maxima along the axis. The relative concentration profile can be self-preserving only if the ratio of the half-widths, $m(s) = \frac{f_{.s_0}}{f_{.s_u}} + \frac{f_{.s_u}}{f_{.s_u}}$ becomes constant for increasing values of $\frac{f_{.s_0}}{f_{.s_u}} + \frac{f_{.s_u}}{f_{.s_u}}$ This is not the case in the experimental data of Laats and Frishman (1970) so that the particulate concentration profile does not become self-preserving.

It has been seen that the particle mass flux attains a self-preserving form but the fluid velocity and particulate concentration do not. Since the product of the particulate concentration and velocity, which has been shown to be virtually the same as the fluid velocity, is the flux, it is apparent that the deviations of the concentration and velocity from similarity balance each other. Lasts and Frishman (1970) observed that for fine particles the width of the concentration profile increases with increasing axial position whereas the opposite occurs for coarse particles.

The deformation of the velocity profile from similarity is attributed to the momentum transport between

the two phases. Since the jet entrains ambient fluid and the velocities of the two phases are nearly the same, conservation of the total momentum within the jet dictates that in the far field essentially all of the momentum is carried in the fluid phase. The momentum transfer is greatest near the axis and diminishes near the edge of the jet [c.f. Laats and Frishman (1970)]. Since the net momentum transfer is from the particles, it is expected that the particle size and concentration should be influential in determining the rate of transfer. The data of Laats and Frishman (1970) confirm this and reveal that the rate of momentum transfer increases with initial particle loading, %, and with decreasing particle size. In addition to supplying a source for momentum transfer between phases, the particles also tend to decrease the turbulent momentum transport across the jet, thereby retarding the rate of particulate diffusion and the spreading rate of the jet.

VII. CONCLUSIONS AND RECOMMENDATIONS

After examining the literature available for twophase flows, it is readily seen that the actual flow is
much more complicated than the treatment given it here.

It is possible, however, that for light loadings of
fine particles the gross features, such as the spreading
rate of the jet and the profiles of the mean velocity and
particulate concentration, may be approximated by the
inclusion of "added dissipation" terms in the 7-k-£ model
as discussed earlier. Since the deformation from similarity of the mean velocity and particulate concentration
profiles are not large in experiments with heavily loaded
jets [Laats and Fishman (1970)], the deformation becomes
unobservable in experiments with lightly loaded jets
[Melville and Bray (1979a)].

Although the profiles in lightly loaded jets appear to become self-preserving, the present modelling terms do not permit a self-preserving form of the equations in the modified 7-k-£ model. Consequently, a solution in the self-preserving region is not obtainable with this model for two-phase jets. An algorithm to solve partial differential equations is therefore required to obtain down-stream profiles. The absence of a similarity solution is

not considered to be a great hindrance to applications of models of two-phase jets to physical systems, however, since most of the applications of two-phase flow, such as coal combustors, occur in the developing region of the jets.

The Tk-f model for single-phase jets gives reasonable results for the predicted profiles of the mean axial velocity and contaminant concentration as well as the turbulence kinetic energy and the square of the root-mean-square contaminant concentration fluctuations.

However, the need to modify the set of constants to achieve a better fit to experimental data for different geometries indicates the absence of a sufficiently complete physical representation of the turbulence. The most serious result of the incompleteness of the model is the behavior of the predicted spreading rate in the plane and axisymmetric jets. The model predicts that the axisymmetric jet spreads faster than the plane jet although the opposite is observed in the actual flows.

Since the proposed modifications to the set of constants used in the model are empirical [c.f. Pope (1978)], their use prohibits the desired universality of the constants. Consequently, the use of sets of constants that best fit the experimental data of a given flow geometry are recommended for the model in its present

state of development if the model is to be extended to two-phase flows.

REFERENCES

- Abramovich, G. N. and Girshovich, T. A. 1974 "Diffusion of Heavy Particles in Turbulent Gas Streams," Soviet Physics-Doklady, 18, 587-589.
- Bashir, J. 1973 Experimental Study of the Turbulent Structure and Heat Transfer of a Two Dimensional Heated Jet. (Unpublished doctoral dissertation, University of Colorado.)
- Becker, H. A., Hottel, H. C., and Williams, G. C. 1967
 "The Nozzle-Fluid Concentration Field of the Round,
 Turbulent, Free Jet." J. Fluid Mech., 30, 285-303.
- Bradbury, L. J. S. 1965 "The Structure of a Self-Preserving Turbulent Plane Jet." J. Fluid Mech., 23, 31-64.
- Chen, C. J. and Rodi, W. 1975 "A Mathematical Model of Stratified Turbulent Flows and its Application to Bouyant Jets." Int. Assoc. for Hydraulic Res., 3, No. 16, 31-37.
- Danon, H.; Wolfshtein, M.; and Hetsroni, G. 1977 "Numerical Calculations of Two-Phase Turbulent Round Jet."

 Int. J. Multiphase Flow, 3, 223-234.
- Fenton, D. L. and Stukel, J. J. 1976 "Flow of a Particulate Suspension in the Wake of a Circular Cylinder." Int. J. Multiphase Flow, 3, 123-139.
- Hanjalic, K. and Launder, B. E. 1972 "A Reynolds Stress Model of Turbulence and its Application to Thin Shear Flows." J. Fluid Mech., 52, 609-638.
- Hinze, J. O. 1972 "Turbulent Fluid and Particle Interaction." Prog. Heat Mass Transfer, 6, 433-452.
- . 1975 <u>Turbulence</u>. McGraw-Hill, New York, 2nd ed.
- Keller, H. B. 1974 "Accurate Difference Methods for Nonlinear Two-Point Boundary Value Problems." SIAM J. Numer. Anal., 11, 305-320.

- Laats, M. K. and Frishman, F. A. 1970 "Assumptions Used in Calculating the Two-Phase Jet." Fluid Dynamics, 5, 333-338.
- Launder, B. E. 1976 "Heat and Mass Transport." in Turbulence, ed. P. Bradshaw, Springer-Verlag. 231-287.
- Launder B. E. and Morse, A. 1977 "Numerical Prediction of Axisymmetric Free Shear Flows With a Second-Order Reynolds Stress Closure." Symposium on Turbulent Shear Flows, Pennsylvania State University, 4.21-4.30.
- Launder, B. E.; Morse, A. P.; Rodi, W.; and Spalding, D. B. 1972 "The Prediction of Free Shear Flows A Comparison fo Six Turbulence Models." NASA SP-311.
- Launder, B. E.; Reece, G. J.; and Rodi, W. 1975 "Progress in the Development of a Reynolds-Stress Turbulence Closure." J. Fluid Mech., 68, 537-566.
- Melville, W. K. and Bray, K. N. C. 1979a "The Two-Phase Turbulent Jet." Int. J. Heat Mass Transfer, 22, 279-287.
- . 1979b "A Model of the Two-Phase Turbulent Jet."

 Int. J. Heat Mass Transfer, 22, 647-656.
- Owen, P. R. 1969 "Pneumatic Transport." J. Fluid Mech., 39, 407-432.
- Pope, S. B. 1978 "An Explanation of the Turbulent Round-Jet/Plane-Jet Anomaly." AIAA Journal, 16, 279-281.
- Reynolds, W. C. 1976 "Computation of Turbulent Flows."

 Ann. Rev. of Fluid Mech., 8, 183-208.
- Rodi, W. and Spalding, D. B. 1970 "A Two-Parameter Model of Turbulence and its Application to Free Jets." Warme-und Stoffubertragung Bd., 3, 85-95.
- Rotta, J. C. 1975 "Prediction of Turbulent Shear Flow Using the Transport Equations for Turbulence Energy and Turbulence Length Scale." Lecture Ser. No. 76, von Karman Inst., Belgium.
- Spalding, D. B. 1971 "Concentration Fluctuations in a Round Turbulent Free Jet." Chem. Eng. Sci., 26, 95-107.

- Wood, P. E. 1978 Studies of Mean Reynolds Stress Models of Turbulent Flow. (Unpublished doctoral dissertation, California Institute of Technology.)
- Wygnanski, I. and Fiedler, H. 1969 "Some Measurements in the Self-Preserving Jet." J. Fluid Mech., 38, 577-612.